

## $\alpha_2$ -Adrenoreceptors Profile Modulation. 2.<sup>1</sup> Biphenylene Analogues as Tools for Selective Activation of the $\alpha_{2C}$ -Subtype

Francesco Gentili,<sup>†</sup> Francesca Ghelfi,<sup>†</sup> Mario Giannella,<sup>†</sup> Alessandro Piergentili,<sup>†</sup> Maria Pignini,<sup>\*,†</sup> Wilma Quaglia,<sup>†</sup> Cristian Vesprini,<sup>†</sup> Pierre-Antoine Crassous,<sup>‡</sup> Hervé Paris,<sup>‡</sup> and Antonio Carrieri<sup>§</sup>

Dipartimento di Scienze Chimiche, Università degli Studi di Camerino, Via S. Agostino 1, 62032 Camerino, Italy, INSERM Unit 388, Institut Louis Bugnard, IFR31, CHU Rangueil, 1 avenue Jean Poulhes, 31403 Toulouse, France, and Dipartimento Farmaco-Chimico, Università degli Studi di Bari, Via E. Orabona 4, 70125 Bari, Italy

Received March 31, 2004

A series of derivatives structurally related to biphenylene (**3**) was designed with the aim to modulate selectivity toward the  $\alpha_2$ -AR subtypes. The results obtained demonstrated that the presence of a correctly oriented function with positive electronic effect (+ $\sigma$ ) in portion X of the ligands is an important factor for significant  $\alpha_{2C}$ -subtype selectivity (imidazolines **5**, **13**, **16**, and **19**). Homology modeling and docking studies support experimental data and highlight the crucial role for the hydrogen bond between the pyridine nitrogen in position 3 of **5** and the NH-indole ring of Trp6.48, which is favorably oriented in the  $\alpha_{2C}$ -subtype, only.

### Introduction

Adrenoreceptors (ARs) play a crucial role in the regulation of a large panel of biological functions and have been considered for many years as attractive therapeutic targets for the treatment of various diseases, such as hypertension, congestive heart failure, asthma, depression, and glaucoma.<sup>2</sup> Chemically and pharmacologically speaking, ARs are membrane proteins belonging to the superfamily of G-protein-coupled receptors<sup>3–5</sup> and are classified into three classes, namely,  $\alpha_1$ -,  $\alpha_2$ -, and  $\beta$ -ARs,<sup>6</sup> which are respectively coupled to proteins G<sub>q</sub>, G<sub>i/o</sub>, and G<sub>s</sub>. As a result of the combined development of radioligand binding assays and molecular biology techniques, it became evident that each class of AR is heterogeneous. In particular, three distinct  $\alpha_2$ -AR subtypes (namely  $\alpha_{2A}$ -,  $\alpha_{2B}$ -, and  $\alpha_{2C}$ -ARs) that are encoded by different genes have been characterized in different species.<sup>7</sup>  $\alpha_2$ -AR subtypes exhibit a high degree of homology and share common mechanisms of signal transduction. They are all involved in the control of the cardiovascular and central nervous systems, although they mediate different functions.<sup>8</sup>

So far, the attribution of a physiological function to a given  $\alpha_2$ -AR subtype has, however, been of great difficulty *in vivo*, due to the lack of sufficiently subtype-selective pharmacological tools. Indeed, while somewhat subtype-discriminative antagonists exist, such as BRL 44408 and BRL 48962 for  $\alpha_{2A}$ ;<sup>9,10</sup> imiloxan, ARC-239, and several *N*-pyrimidinyl-4-aminobenzenesulfonamide derivatives for  $\alpha_{2B}$ ;<sup>11–13</sup> and rauwolscine and MK 912 for  $\alpha_{2C}$ ,<sup>6,14</sup> although with significant limitations both relating to poor selectivity and affinity for other neurotransmitter receptors (e.g.  $\alpha_1$ -ARs for ARC-239 and various 5-HT subtypes for rauwolscine), no strictly selective agonists are available yet for  $\alpha_{2B}$ - and  $\alpha_{2C}$ -ARs. Furthermore, even though oxymethazoline, whose use

is limited by its potent agonist activity at  $\alpha_1$ -ARs, and guanfacine<sup>15</sup> display a significant preference for  $\alpha_{2A}$ -AR, the selectivity of the available agonists is far from being sufficient for a complete *in vivo* characterization of the three  $\alpha_2$ -AR subtypes.

The establishment of genetically engineered mice lacking or overexpressing  $\alpha_2$ -AR subtypes<sup>16</sup> has yielded important information for understanding the subtype-specific functions. Genetic manipulation has been of great help, but at the same time it presents limitations insofar that significant evolutionary changes can sometimes compensate for the loss of the targeted gene. However, as recently reviewed,<sup>17</sup> the examination of the phenotype of these strains of mice demonstrated that the  $\alpha_{2A}$  subtype is responsible for inhibition of neurotransmitter release from central and peripheral sympathetic nerves and for most of the centrally mediated effects of  $\alpha_2$ -agonists, including hypotension,<sup>18</sup> anesthesia,<sup>19</sup> sedation,<sup>19,20</sup> antiepileptogenesis,<sup>21</sup> and analgesia.<sup>19,20,22</sup> Further data suggested that stimulation of the postsynaptic  $\alpha_{2A}$ -AR increases the blood flow in the prefrontal cortex and enhances the working memory functions, as treatment with the  $\alpha_{2A}$  agonist guanfacine significantly improves cognitive performance.<sup>23</sup>

The  $\alpha_{2B}$ -AR is primarily responsible for the initial peripheral hypertensive responses evoked by the  $\alpha_2$ -agonists<sup>24</sup> and takes part in the hypertension induced by salt.<sup>25</sup>

Clarification of the physiological role of  $\alpha_{2C}$  subtype proved more difficult.<sup>16</sup> Despite a rather wide distribution in the central nervous system, its role did not appear critical in the mediation of the cardiovascular effects of nonselective  $\alpha_2$ -agonists.<sup>24</sup> Its participation has been suggested in the hypothermia induced by dexmedetomidine and in the hyperlocomotion induced by D-amphetamine.<sup>26</sup> Another potentially important response mediated by the  $\alpha_{2C}$ -AR is constriction of cutaneous arteries, leading to a reduction in cutaneous blood flow.<sup>27</sup> Recent studies carried out on double knockout mice have suggested that  $\alpha_{2C}$ -AR is also expressed at the presynaptic level where, together with  $\alpha_{2A}$ , it

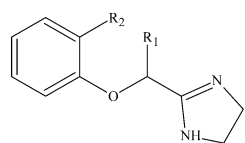
\* To whom correspondence should be addressed. Phone: +39 0737 402237. Fax: +39 0737 637345. E-mail: maria.pignini@unicam.it.

<sup>†</sup> Università degli Studi di Camerino.

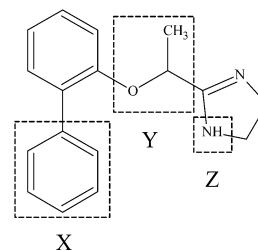
<sup>‡</sup> Institut Louis Bugnard.

<sup>§</sup> Università degli Studi di Bari.

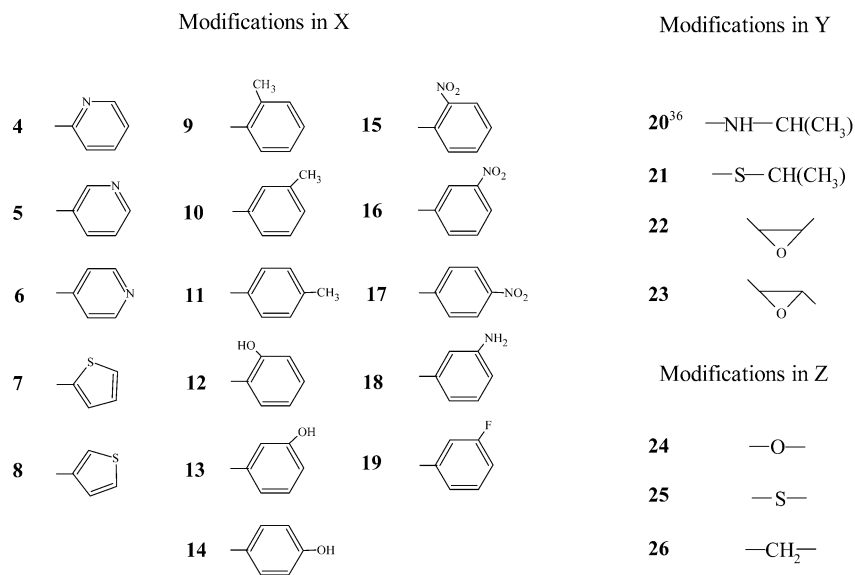
Chart 1



- 1,  $R_1=R_2=H$   
 2,  $R_1=CH_3$ ;  $R_2=H$   
 3,  $R_1=CH_3$ ;  $R_2=C_6H_5$  (Biphenylene)



4-26



actively participates in the control of neurotransmitter release. However, the two subtypes regulate this process differently. Indeed, while  $\alpha_{2A}$ -AR is particularly efficient at high stimulation frequencies,  $\alpha_{2C}$ -AR acts rather at low stimulation frequencies.<sup>28</sup> Moreover, it has been suggested that  $\alpha_{2C}$  subtype participates in the modulation of motor behavior and the memory processes.<sup>29,30</sup> Other central effects triggered by this subtype include also the startle reflex and aggression,<sup>31</sup> response to stress, and locomotion.<sup>32</sup> Last, it was recently pointed out that the  $\alpha_{2C}$ -AR may contribute to  $\alpha_2$ -agonist-mediated spinal analgesia and adrenergic-opioid synergy.<sup>33</sup>

Previous studies from our group have demonstrated that modest structural modifications within imidazoline molecules resulted in significant alteration in their affinity, both with regard to different receptor systems and inside the same system, with resultant enhanced selectivity.<sup>34-37</sup>

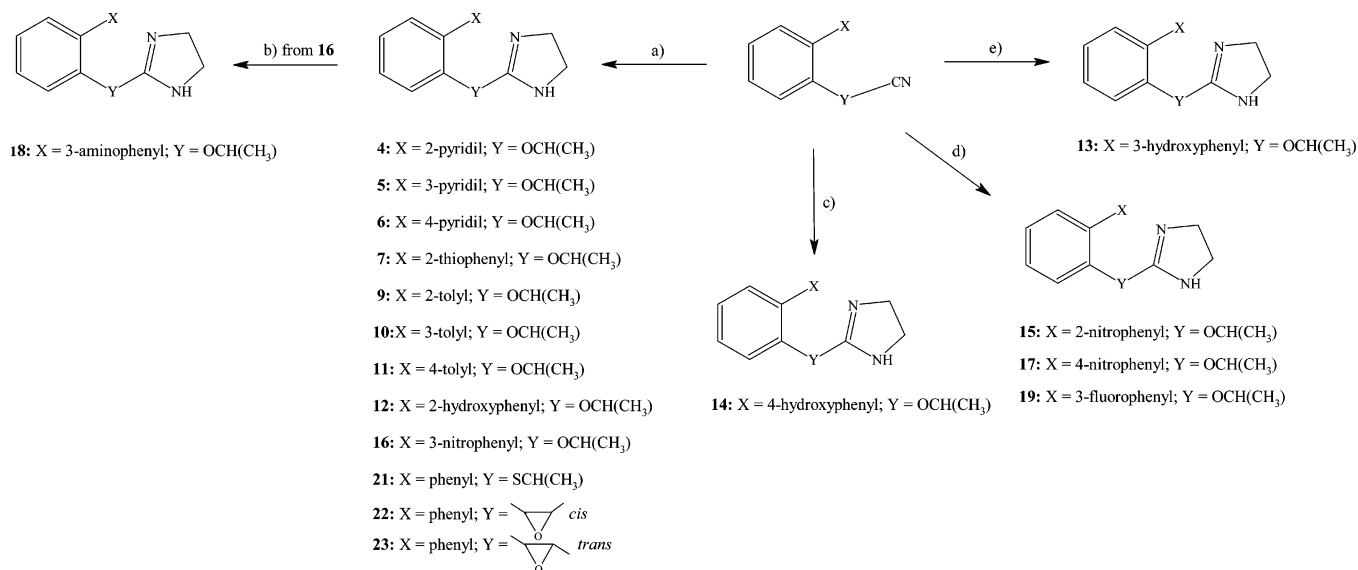
In the context of the  $\alpha_2$ -AR system, a very interesting result was obtained by modifying the basic structure of 2-phenoxymethylimidazoline (**1**) by the successive introduction of a methyl substituent in the oxymethylene bridge (compound **2**) and of a phenyl group in the ortho position of the aromatic ring (2-[1-(biphenyl-2-yloxy)ethyl]-4,5-dihydro-1*H*-imidazole, compound **3**) (Chart 1). The name of biphenylene has now been given to compound **3**.

Imidazolines **1** and **2** both behaved as antagonists at  $\alpha_2$ -ARs and as weak agonists at  $\alpha_1$ -ARs but exhibited a

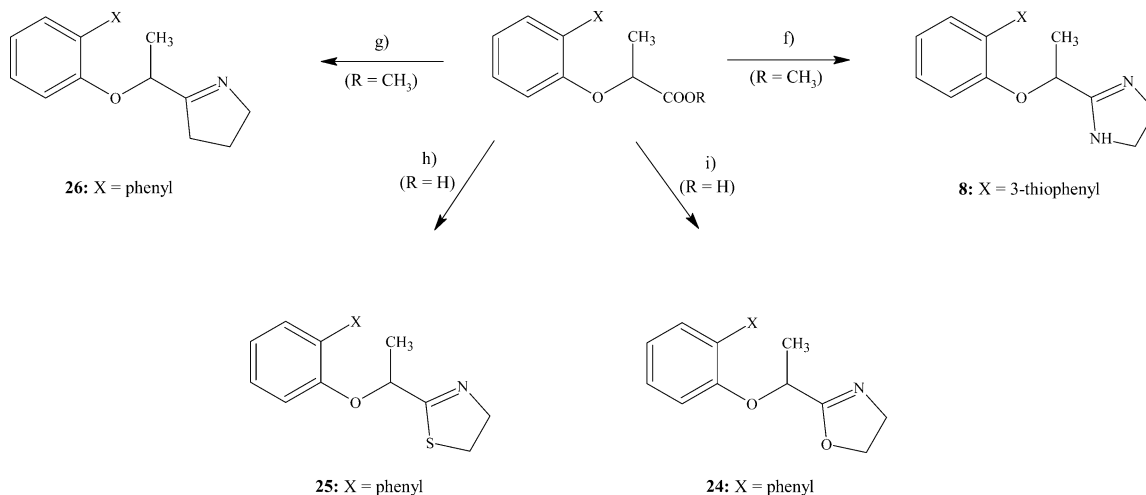
very different affinity profile toward  $I_2$ -imidazoline binding sites ( $I_2$ -IBS), with compound **1** having high affinity ( $pK_i I_2 = 9.05$ ) and compound **2** low affinity ( $pK_i I_2 = 5.57$ ).<sup>36</sup> The methyl group on the bridge reduced the  $\alpha_1$ -adrenergic intrinsic activity and moderately enhanced the  $\alpha_2$ -adrenergic potency (methyl binding pocket recognition)<sup>38</sup> but overall markedly decreased the  $I_2$ -IBS affinity.<sup>36,37</sup> Interestingly, compounds **1** and **2** also displayed significant  $\alpha_2$ -adrenergic selectivity toward the  $I_1$ -IBS.<sup>37</sup>

Since the structural characteristics of numerous ligands of  $\alpha_2$ -ARs (such as clonidine, oxymethazoline, idazoxan, and rilmenidine)<sup>39,40</sup> are compatible with the architecture of the imidazoline binding sites, the reduction of their affinity toward IBS can be useful for improving the selectivity of drugs that can potentially be employed for treating various diseases.

As expected, biphenylene (**3**) exhibited an interesting  $\alpha_2$ -adrenergic selectivity profile [ $pK_i \alpha_2 = 7.91$ ;  $pK_i I_1 = 6.90$  (unpublished result);  $pK_i I_2 = 5.79$ ], but rather surprisingly, it behaved as an efficient  $\alpha_2$ -agonist in vitro assays on isolated rat vas deferens. It is probable that the phenyl substituent introduced in the ortho position of the aromatic ring is able to form  $\pi$ - $\pi$  stacking interactions with the aromatic cluster of the binding cavity, therefore playing an important role in  $\alpha_2$ -AR activation. Moreover, the biphenylene eutomer (*S*)-(-) displayed enhanced and long-lasting antinociceptive potency, undoubtedly mediated by the  $\alpha_2$ -AR since

Scheme 1<sup>a</sup>

<sup>a</sup> Reagents: (a) CH<sub>3</sub>ONa, CH<sub>3</sub>OH/H<sub>2</sub>NCH<sub>2</sub>CH<sub>2</sub>NH<sub>2</sub>; (b) H<sub>2</sub>, Pd/C; (c) HCl(g), CH<sub>3</sub>OH/H<sub>2</sub>NCH<sub>2</sub>CH<sub>2</sub>NH<sub>2</sub>; (d) H<sub>2</sub>NCH<sub>2</sub>CH<sub>2</sub>NH<sub>2</sub>/Δ; (e) H<sub>2</sub>NCH<sub>2</sub>CH<sub>2</sub>NH<sub>3</sub><sup>+</sup>·*p*TSA/Δ.

Scheme 2<sup>a</sup>

<sup>a</sup> Reagents: (f) (CH<sub>3</sub>)<sub>3</sub>Al/dry toluene; H<sub>2</sub>NCH<sub>2</sub>CH<sub>2</sub>NH<sub>2</sub>/Δ; (g) NaH, *N*-vinyl-2-pyrrolidinone; (h) HSCH<sub>2</sub>CH<sub>2</sub>NH<sub>2</sub>, Ph<sub>3</sub>P, Et<sub>3</sub>N/Δ; (i) oxalyl chloride, Et<sub>3</sub>N/HOCH<sub>2</sub>CH<sub>2</sub>NH<sub>2</sub>; SOCl<sub>2</sub>; Et<sub>3</sub>N.

it was competitively blocked by the selective α<sub>2</sub>-antagonist, RX 821002.<sup>36</sup>

The biological activity and the pharmacological profile of biphenylene therefore encouraged us to synthesize a new series of derivatives with the aim to improve both potency and α<sub>2</sub>-AR subtype selectivity. In the present study, chemical modifications have been designed at the level of the portions X, Y, and Z of the lead molecule **3**. The properties of these new compounds **4–19**, and **21–26** (Chart 1) were evaluated by binding and functional studies using human α<sub>2</sub>-AR subtypes expressed in Chinese hamster ovary (CHO) cells.

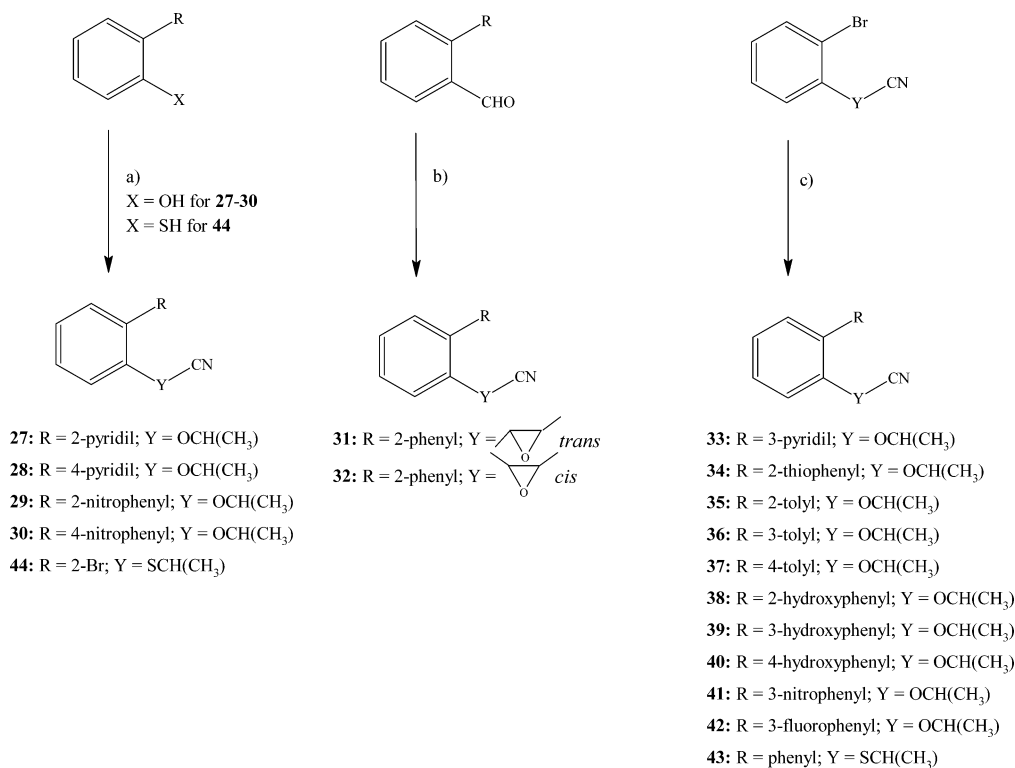
## Chemistry

Compounds **4–7**, **9–17**, **19**, and **21–23** were synthesized according to standard methods by condensation of suitable nitriles with ethylenediamine. Amino derivative **18** was obtained through catalytic hydrogenation of **16** over Pd/C (Scheme 1).

Imidazolines **8** and **26** were obtained from 2-(2-thiophen-3-yl-phenoxy)- (**46**) and 2-(biphenyl-2-yloxy)pro-

pionic acid methyl ester<sup>36</sup> by treatment with ethylenediamine in the presence of trimethylaluminum or by treatment with 1-vinyl-2-pyrrolidinone in the presence of NaH, respectively. Reaction of 2-(biphenyl-2-yloxy)propionic acid<sup>41</sup> with 2-aminoethanethiol in the presence of triphenylphosphine provided compound **25**, and that with ethanolamine in the presence of oxalyl chloride and triethylamine yielded compound **24** (Scheme 2).

The intermediate nitriles were prepared according to Scheme 3 starting from 2-chloropropionitrile and the suitable phenols for **27–30**<sup>42,43</sup> or thiophenol for **44**, from 2-(2-bromophenoxy)propionitrile and the suitable commercially available boronic acids in the presence of tetrakis(triphenylphosphine)palladium(0) for **33–42**, and from 2-(2-bromophenylsulfanyl)propionitrile (**44**) and phenylboronic acid for **43**. Finally, nitriles **31** and **32** were prepared as a *trans/cis* mixture (ratio 6:3) from 2-biphenylcarboxaldehyde and chloroacetonitrile in the presence of *t*-ButOK. The two isomers **31** and **32** were separated by flash chromatography. The stereochemical relationship between the CN function at position 2 and

Scheme 3<sup>a</sup>

<sup>a</sup> Reagents: (a) 2-chloropropionitrile, K<sub>2</sub>CO<sub>3</sub>, DME; (b) t-BuOK, t-BuOH/chloroacetonitrile; (c) arylboronic acid, K<sub>2</sub>CO<sub>3</sub>, Pd[(C<sub>6</sub>H<sub>5</sub>)<sub>3</sub>P]<sub>4</sub>.

the 3-biphenyl group was deduced from the coupling constants of the hydroxy atoms at the same positions.<sup>44</sup>

**Pharmacology.** The pharmacological profile of compounds was investigated using stable clones of Chinese hamster ovary cells expressing the human  $\alpha_2$ -AR subtypes individually.<sup>45</sup> Binding experiments were carried out on crude membrane preparations using [<sup>3</sup>H]RX 821002 as radioligand.<sup>46</sup> The IC<sub>50</sub> values were determined by nonlinear regression analysis of competition data using the Graphpad Prism computer program. K<sub>i</sub> values were calculated from the equation of Cheng and Prusoff<sup>47</sup> and reported as pK<sub>i</sub> ± SEM.

Agonist potency, defined as the concentration that produces 50% of the maximum response, is expressed as pEC<sub>50</sub> and was determined by use of a cytosensor microphysiometry instrument on the above-mentioned CHO cells. With this instrument, the rate of extracellular acidification after stimulation of the receptor by the agonist was measured.<sup>48</sup> The intrinsic activity (ia) of each compound is expressed as the fraction of the maximum response elicited by (–)-noradrenaline (ia = 1).

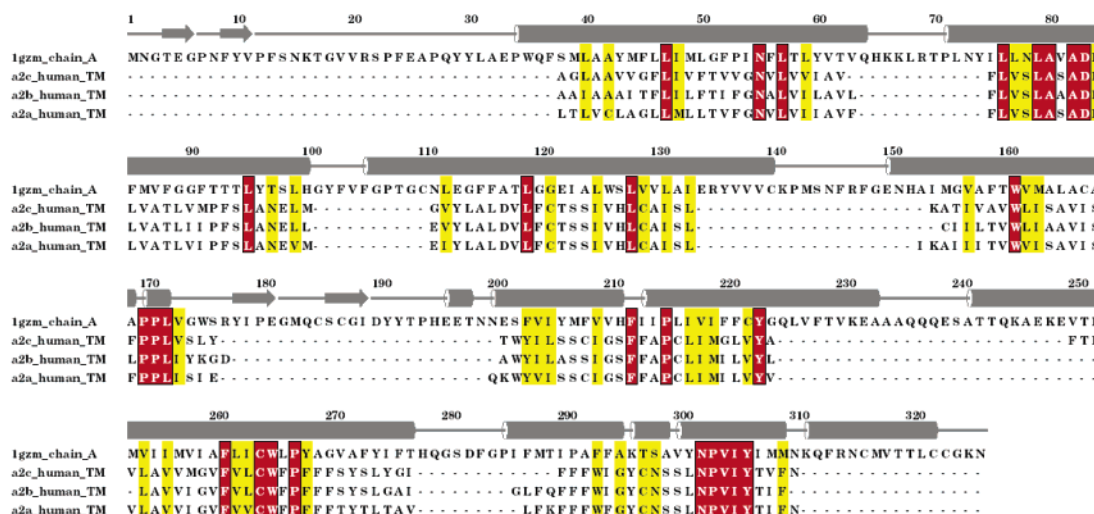
**Modeling. Numbering of Residues.** Residues were numbered according to their positions in the human  $\alpha_2$ -AR sequences, as reported in the SwissProt sequence database.<sup>49</sup> Also residues were indexed according to the numbering proposed by Ballesteros and Weinstein.<sup>50</sup> The *transmem* annotation of the sequence file was taken into account as a definition of the amino acids comprising the seven transmembrane helices (TMs).

**Model Building.** The TM models of each  $\alpha_2$ -AR subtype were built by starting from the X-ray structure of the bovine rhodopsin, which has been recently solved by Schertler et al.<sup>51</sup> Despite low sequence identity between the selected template and the three receptors

(~20%), bovine rhodopsin still represents a reliable template once a transmembrane receptor has to be modeled; it is in fact the only eukaryotic G-protein-coupled receptor (GPCR) whose typical folding, represented by a seven  $\alpha$ -helix domain spanning through the cell membrane connected by extracellular and intracellular loops, has been experimentally determined; in addition, the percentage of identity of bovine rhodopsin with the  $\alpha_2$ -ARs rises up to ~30% when considering only the transmembrane domain. The homology modeling tool MODELLER<sup>52</sup> (ver. 6.2) was used to assemble and refine the seven TM framework. Loops were not taken into account, mainly since they do not directly interact in the binding of ligands showing an agonist profile, at least in the case of the aminergic receptors family, and also to avoid a very hard risking phase in the homology building procedure due to the low sequence identity with the selected template. The Cartesian coordinates of the C $\alpha$  atoms relative to the  $\alpha_2$ -ARs were copied from the corresponding ones of the selected template (PDB code 1gzm, chain A) according to the sequence alignment reported in Figure 1.

Five hundred different 3D structures were generated using the slow molecular dynamic optimization schedule *refine\_3*. To ensure a complete investigation of the tertiary structure, side chains were fully randomized in a range of ±180°. The models obtained were then superposed and clustered according to their C $\alpha$  position by means of the NMRCLUST algorithm;<sup>53</sup> no predefined root mean square threshold was applied during the clustering procedure. For each  $\alpha_2$ -AR subtype, the model exhibiting the lowest potential density function value, as scored by MODELLER, was selected as input structure in the docking studies, since it was also a member of the most populated cluster. To better assess the





**Figure 1.** Pairwise alignment of the bovine rhodopsin sequence and the human  $\alpha_2$ -adrenergic receptors. The conserved residues are in red boxes. Bars indicate  $\alpha$ -helices and the  $\beta$ -sheet of the selected template. Numbering is referred to rhodopsin.

quality of the chosen structures, the stereochemical parameters were checked by means of the PROCHECK software;<sup>54</sup> in all three cases, the percentage of the residues lying in the most favored regions of the Ramachandran plot was more than 90%.

**Molecular Docking.** The molecular structure of compound **5** was built using standard bond lengths and angle valences implemented in the latest Flo+ software library.<sup>55</sup> The imidazoline ring was protonated and the absolute (*S*) configuration was arbitrarily selected in agreement with the highest biological activity of the same enantiomer of the biphenylene (**3**), as previously measured.<sup>36</sup> In fact, docking performed using the absolute (*R*) configuration highlighted considerably different interactions for the enantiomers, in agreement with the measured biological data. The mixed AMBER/MM2 force field of the same software package was used for geometry optimization and energy calculation. Flexible docking of compound **5** to the  $\alpha_2$ -ARs binding site was performed first by means of the DYNDOCK module of Flo+. This algorithm operates by randomly rotating and translating the ligand within the receptor binding site, perturbing at the same time its internal geometry with respect to the dihedral angles, according to the Monte Carlo algorithm. At each step, a short dynamic run followed by a Pollak–Ribiere conjugate gradient minimization was performed on the receptor–ligand complex. A single distance constraint between the protonated nitrogen of the imidazoline ring and the carboxy group of Asp3.32 was applied, because site-directed mutagenesis experiments have previously demonstrated that this residue is responsible for the anchoring of natural agonists (i.e. noradrenaline) to the binding site.<sup>56</sup> In our case, the ligand was initially placed in the receptor binding cavity located within TM3, -5, -6, and -7. The receptor–ligand complex was first minimized and then subjected to 100 steps of flexible dynamic docking performed keeping the C $\alpha$  trace of the receptor fixed to the initial position. The receptor–ligand complex having the best energy of binding according to the Flo+ scoring function was then selected for a further 3000 steps of Monte Carlo docking simulation performed with the MCDOCK+ module. This time, only the ligand and the amino acid residues lying in a closer distance

range to the agonist structure were allowed to move (Table 4).

**Computing.** MODELLER calculations were run on a DELL Pentium IV 2.56 GHz, whereas docking studies were carried out on a SGI Origin300 R14000.

## Results and Discussion

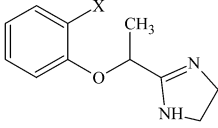
Tables 1–3 report the affinity values, potency, and intrinsic activity of the new compounds and biphenylene (**3**); compound **20**<sup>36</sup> was also included in the present study for a more complete structure–activity relationship investigation. None of the compounds were evaluated for their antagonist activity.

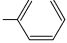
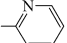
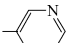
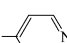
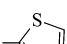
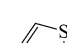
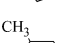
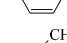
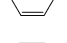
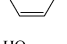
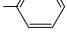
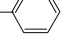
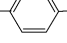
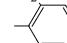
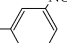
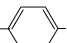
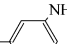
The results show that biphenylene (**3**) behaves as a good agonist with comparable potency and affinity toward the  $\alpha_{2A}$  and  $\alpha_{2C}$  subtypes but as a partial agonist with modest intrinsic activity toward the  $\alpha_{2B}$ -subtype.

Since the phenyl group in the ortho position of the aromatic ring was already hypothesized as being responsible for the biphenylene  $\alpha_2$ -agonist property,<sup>36</sup> the main objective of the present study was to verify the consequences of modifications affecting this portion of the molecule. These modifications included (i) isosteric substitution with the pyridine nucleus (compounds **4–6**) and thiophene nucleus (compounds **7–8**) and (ii) introduction in the ortho, meta, and para positions of the phenyl group of substituents with different  $\sigma$  and  $\pi$  contributions (compounds **9–19**) (modifications in X, Chart 1).<sup>57</sup> All the new derivatives exhibited pK<sub>i</sub> values similar to that of biphenylene and generally displayed higher affinity for  $\alpha_{2A}$  or  $\alpha_{2C}$  than for  $\alpha_{2B}$  subtype. The most interesting point was that they showed considerable and selective modulation of their functional activity toward the different subtypes (Table 1).

The introduction of the methyl substituent in ortho, meta, and para positions (for which the  $-\sigma$  and  $+\pi$  condition was verified) led to derivatives **9–11**. Although likely due to an incompatible steric hindrance, none of the three compounds was active at  $\alpha_{2A}$ - or  $\alpha_{2B}$ -AR, but all three behaved as partial agonists with weak potency at  $\alpha_{2C}$ -AR, suggesting agonist selectivity for this subtype with respect to the others.

The effects produced by introducing the hydroxyl group were more dramatic. In fact, whereas the ortho

**Table 1.** Potency ( $pEC_{50}^a$ ), Intrinsic Activity ( $ia^b$ ), and Binding Data ( $pK_i^c$ ) of Compounds **3–19** on Human  $\alpha_2$ -AR Subtypes


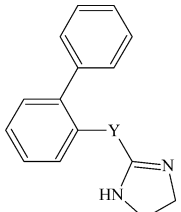
compd	X	$\alpha_{2A}$			$\alpha_{2B}$			$\alpha_{2C}$		
		$pK_i$	$pEC_{50}$	ia	$pK_i$	$pEC_{50}$	ia	$pK_i$	$pEC_{50}$	ia
<b>3</b> Biphenylene		7.32±0.08	6.94±0.06	0.70	6.30±0.07	6.19±0.11	0.50	6.70±0.04	7.24±0.01	0.80
<b>4</b>		5.92±0.05	NA		5.48±0.18	NA		5.90±0.10	NA	
<b>5</b>		6.86±0.05	6.50±0.09	0.50	6.03±0.04	6.00±0.09	0.50	7.19±0.04	7.30±0.16	1.00
<b>6</b>		6.55±0.12	NA		5.57±0.05	NA		5.84±0.28	NA	
<b>7</b>		7.77±0.04	7.38±0.10	0.80	6.67±0.10	6.00±0.21	0.60	7.14±0.06	7.23±0.05	0.80
<b>8</b>		7.34±0.02	7.12±0.08	0.70	6.38±0.04	NA		6.88±0.07	7.03±0.28	0.85
<b>9</b>		7.33±0.00	NA		6.08±0.07	NA		6.63±0.03	6.44±0.32	0.45
<b>10</b>		7.29±0.02	NA		6.27±0.01	NA		6.61±0.08	5.80±0.29	0.60
<b>11</b>		7.38±0.03	NA		6.40±0.08	NA		6.60±0.06	6.08±0.17	0.46
<b>12</b>		6.51±0.09	NA		6.00±0.05	NA		5.79±0.02	NA	
<b>13</b>		7.56±0.02	NA		6.45±0.01	5.28±0.17	0.50	7.75±0.08	7.33±0.15	1.15
<b>14</b>		7.47±0.08	NA		6.09±0.09	NA		6.48±0.09	NA	
<b>15</b>		6.76±0.00	NA		5.81±0.20	NA		5.91±0.04	NA	
<b>16</b>		7.22±0.03	NA		6.18±0.08	NA		6.63±0.08	7.00±0.09	0.60
<b>17</b>		6.91±0.06	NA		6.30±0.02	NA		6.52±0.13	NA	
<b>18</b>		7.43±0.08	6.59±0.21	0.45	6.32±0.09	NA		6.51±0.01	6.30±0.18	0.50
<b>19</b>		7.83±0.03	6.98±0.09	0.58	6.57±0.07	NA		7.77±0.04	7.22±0.16	1.15
<b>(-)-Noradrenaline</b>			6.43±0.17	1.00		7.21±0.25	1.00		6.10±0.05	1.00

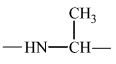
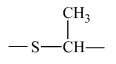

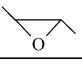
<sup>a</sup> Determined by applying the cytosensor microphysiometry system<sup>48</sup> to study the three human  $\alpha_2$ -AR subtypes,  $\alpha_{2A}$ ,  $\alpha_{2B}$ ,  $\alpha_{2C}$ , expressed in Chinese hamster ovary (CHO) cells and to assess its potential in the quantitative monitoring of agonist activity. The full agonist (-)-noradrenaline was used to define agonist efficacy (ia). NA = not active (ia < 0.3). <sup>b</sup> Intrinsic activity (ia) is the maximum effect obtained with the agonist under study, expressed as percentage of (-)-noradrenaline taken as equal to 1. <sup>c</sup> Binding assays using [<sup>3</sup>H]RX 821002 were performed with membrane preparations from the same cell models.

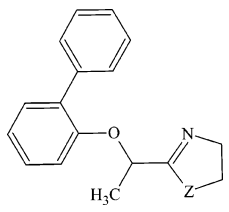
and para derivatives **12** and **14** ( $-\sigma$  and  $-\pi$ ) were functionally inactive at all three  $\alpha_2$ -AR subtypes, the *m*-hydroxy derivative **13** ( $+\sigma$  and  $-\pi$ ) behaved as a full agonist with intrinsic activity equivalent to that of (-)-noradrenaline toward the  $\alpha_{2C}$  subtype ( $pEC_{50} \alpha_{2C} = 7.33$ ,

ia = 1.15). It should be noted that compound **13** was totally inactive at  $\alpha_{2A}$  subtype and produced only a weak and partial activation of the  $\alpha_{2B}$ -AR.

Also interesting were the effects of nitro substitution ( $+\sigma$  and  $-\pi$ ). Indeed, whereas the ortho and para

**Table 2.** Potency (pEC<sub>50</sub><sup>a</sup>), Intrinsic Activity (ia<sup>b</sup>), and Binding Data (pK<sub>i</sub><sup>c</sup>) of Compounds **20–23** on Human α<sub>2</sub>-AR Subtypes


Compd	Y	α <sub>2A</sub>			α <sub>2B</sub>			α <sub>2C</sub>		
		pK <sub>i</sub>	pEC <sub>50</sub>	ia	pK <sub>i</sub>	pEC <sub>50</sub>	ia	pK <sub>i</sub>	pEC <sub>50</sub>	ia
<b>20</b>		7.04±0.07	6.41±0.11	0.70	5.94±0.05	5.42±0.10	0.50	6.15±0.14	7.03±0.03	0.70
<b>21</b>		6.47±0.09	NA		5.45±0.07	NA		6.15±0.03	NA	
<b>22</b>		5.91±0.11	5.46±0.05	0.66	4.70±0.09	NA		5.19±0.22	5.57±0.01	0.73
<b>23</b>		5.82±0.03	NA		5.91±0.08	NA		5.37±0.08	NA	

<sup>a-c</sup> See Table 1.**Table 3.** Potency (pEC<sub>50</sub><sup>a</sup>), Intrinsic Activity (ia<sup>b</sup>), and Binding Data (pK<sub>i</sub><sup>c</sup>) of Compounds **24–26** on Human α<sub>2</sub>-AR Subtypes


compd	Z	α <sub>2A</sub>		α <sub>2B</sub>		α <sub>2C</sub>	
		pK <sub>i</sub>	pEC <sub>50</sub>	pK <sub>i</sub>	pEC <sub>50</sub>	pK <sub>i</sub>	pEC <sub>50</sub>
<b>24</b>	-O-	5.09 ± 0.04	NA	5.00 ± 0.09	NA	5.23 ± 0.01	NA
<b>25</b>	-S-	<5	NA	<5	NA	<5	NA
<b>26</b>	-CH <sub>2</sub> -	5.09 ± 0.04	NA	5.00 ± 0.02	NA	5.23 ± 0.09	NA

<sup>a-c</sup> See Table 1.**Table 4.** Residues Defining the Binding Site in the Human α<sub>2</sub>-ARs

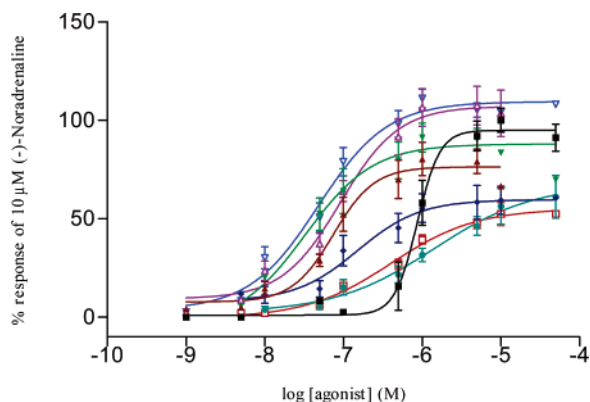
domain	α <sub>2A</sub>	α <sub>2B</sub>	α <sub>2C</sub>
TM3	Asp113, Val114, Phe116 Cys117, Thr118 Ser200, Ser201	Asp92, Val93, Phe95 Cys96, Thr97 Ser176, Ser177,	Asp131, Val132, Phe134 Cys135, Thr136 Ser214, Ser215
TM5	Ser204, Phe205 Phe383, Trp387, Phe390	Ser180, Phe181 Phe380, Trp384, Phe387	Ser218, Phe219 Phe391, Trp395, Phe398
TM6	Phe391, Phe392	Phe388, Phe389	Phe399, Phe400
TM7	Phe412, Gly415, Tyr416	Phe412, Gly415, Tyr416	Phe423, Gly426, Tyr427

isomers **15** and **17** were not able to activate any of the α<sub>2</sub>-AR subtypes, the meta isomer **16** behaved as a partial agonist with substantial activity at α<sub>2C</sub> subtype (pEC<sub>50</sub> α<sub>2C</sub> = 7.00, ia = 0.60) but was inactive toward α<sub>2A</sub> and α<sub>2B</sub> subtypes.

Of the pyridine derivatives, the two isomers **4** and **6** were inactive at all subtypes. By contrast, the regioisomer **5**, in which the nitrogen atom occupies a position analogous to that of the nitro group in the meta position of **16** (the nitrogen atom of the pyridine ring and the nitro group of the aromatic ring possess polarity and similar electron-withdrawing effects), was a full agonist at the α<sub>2C</sub>-AR (pEC<sub>50</sub> α<sub>2C</sub> = 7.30, ia = 1) but exhibited lower potency and intrinsic activity toward α<sub>2A</sub> (pEC<sub>50</sub> α<sub>2A</sub> = 6.50, ia = 0.50) and α<sub>2B</sub> (pEC<sub>50</sub> α<sub>2B</sub> = 6.00, ia = 0.50) subtypes.

The agonist potency of compounds **5** and **16** was determined also as a function of their capacity to inhibit forskolin-induced cAMP accumulation in the CHO cells expressing α<sub>2A</sub>- or α<sub>2C</sub>-AR.<sup>58</sup> The pEC<sub>50</sub> values were fairly similar to those obtained from the measurement of medium acidification (Compound **5**: pEC<sub>50</sub> α<sub>2A</sub> = 6.23, ia 0.50; pEC<sub>50</sub> α<sub>2C</sub> = 7.40, ia = 1. Compound **16**: α<sub>2A</sub> NA; pEC<sub>50</sub> α<sub>2C</sub> = 6.80, ia = 0.60.).

To explain this selectivity and taking as model the pyridine derivative **5**, we hypothesized that the nitrogen atom, equipped with a good density of negative charge, enabled a polar interaction with an electrophilic site of the receptor protein. In other words, the activation of the α<sub>2C</sub>-AR was possible solely when the ligand dipole was correctly oriented (nitrogen in position 3 but not in 2 or 4). Therefore, the introduction of chemical functions



**Figure 2.** Stimulation of extracellular acidification in CHO cells stably expressing the human  $\alpha_{2C}$ -adrenergic subtype by (–)-noradrenaline (■), biphenylene (▲), **5** (▼), **10** (●), **13** (▽), **16** (◆), **18** (□), **19** (△). Data points with error bars represent the mean  $\pm$  SEM of three to six separate experiments.

with a positive electronic effect ( $+\sigma$ ) in position 3 of portion X (Chart 1) can lead to efficient and selective agonists for the  $\alpha_{2C}$  subtype (compounds **5**, **13**, and **16**) (Figure 2). Confirmation of this view was provided by compounds **18** and **19**. In fact, the *m*-fluoro derivative **19** ( $+\sigma$  and  $+\pi$ ) proved to be a full agonist at  $\alpha_{2C}$  ( $pEC_{50} \alpha_{2C} = 7.22$ ,  $ia = 1.15$ ), a partial agonist at  $\alpha_{2A}$  ( $pEC_{50} \alpha_{2A} = 6.98$ ,  $ia = 0.58$ ), but totally inactive at  $\alpha_{2B}$ -subtype. On the other hand, the *m*-amino derivative **18** ( $-\sigma$  and  $-\pi$ ) was only a modest partial agonist unable to discriminate between  $\alpha_{2A}$  and  $\alpha_{2C}$  (Figure 2). Thus, the positive or negative values of  $\pi$  do not appear determinant for the biological profile of the ligands.

The thiophene nucleus, considered to be an electron-rich heterocycle, possesses an aromaticity comparable with that of the phenyl ring; however, its reduced size might make more efficient the  $\pi$ – $\pi$  aromatic stacking interactions. Consequently, derivatives **7** and **8** behaved similarly to biphenylene (**3**). They were good agonists for both the  $\alpha_{2A}$  and  $\alpha_{2C}$  subtypes (Compound **7**:  $pEC_{50} \alpha_{2A} = 7.38$ ,  $ia = 0.80$ ;  $pEC_{50} \alpha_{2C} = 7.23$ ,  $ia = 0.80$ . Compound **8**:  $pEC_{50} \alpha_{2A} = 7.12$ ,  $ia = 0.70$ ;  $pEC_{50} \alpha_{2C} = 7.03$ ,  $ia = 0.85$ ).

In this series of compounds, the study of the bridge (portion Y, Chart 1) showed its critical role for the interaction with  $\alpha_2$ -ARs. Bridge rigidity in an epoxidic ring, a modification resulting in the blockade of free rotation and in the alteration of the correct spatial arrangement of aromatic portion and imidazoline nucleus (compounds **22** and **23**) (Table 2), drastically compromised the affinity and efficacy of the lead. Of the two geometric isomers, only the *cis* derivative **22** weakly activated the  $\alpha_{2A}$ - and  $\alpha_{2C}$ -AR subtypes. In the same manner, the isosteric substitution of the oxygen atom of the bridge was rather prejudicial for activity. Indeed, the amino derivative **20**<sup>36</sup> exhibited similar *ia* but lower *pKi* and  $pEC_{50}$  than biphenylene, while the thio derivative **21** was not active at all. Moreover, we recently verified for structurally correlated compounds that the wholly carbon chain of the bridge tended to favor selectivity for IBS with respect to  $\alpha_2$ -ARs.<sup>37</sup>

Finally, as shown by compounds with modifications in portion Z, the ionic bond between the carboxylate anion of an aspartic acid residue of the protein and the protonated nitrogen of the ligand, which is likely the

driving force in the drug-receptor interaction, was ensured only in the presence of the imidazoline nucleus. In this nucleus, the conjugated acid generated as a consequence of protonation proved to be stabilized by two resonance structures having the same energy content. As already known, the contribution to resonance stabilization of oxygen, sulfur, or carbon atoms to the conjugated acid analogues is more scanty. That may explain the incapacity of the derivatives with oxazoline (**24**), thiazoline (**25**), and pyrroline (**26**) nuclei to bind any of the three  $\alpha_2$ -AR subtypes (Table 3).

Homology modeling and docking studies with compound **5** were undertaken to support our hypothesis. The 3D structure of a receptor or protein built by means of homology modeling is always affected by the intrinsic uncertainty deriving from the several theoretical assumptions and methodological approximations that such a kind of study determines. To assess the quality of any model, it is then essential to examine its performance when the binding of ligands with high affinity or efficacy is simulated. Therefore, to validate our receptor models, the binding of compound **5** was performed by means of fully automated flexible docking algorithms, due to the good  $\alpha_{2C}$ -selectivity that this agonist expresses toward the  $\alpha_{2A}$ - and  $\alpha_{2B}$ -AR subtypes. It is our opinion that if the overall spatial arrangement of a modeled receptor, or at least of its binding site, is correct, then a docking study should be able to detect a proper binding mode for efficacy ligands, showing most of the experimentally known favorable interactions, especially the ones highlighted by site-directed mutagenesis data. Moreover, the better the quality of the models, the higher should be the capability of those models to take into account and properly score the differences, either only qualitatively or also quantitatively, in terms of the experimental data (i.e., affinity or efficacy). To address this topic, the structural features of the complexes obtained by the docking of compound **5** were carefully analyzed and evaluated.

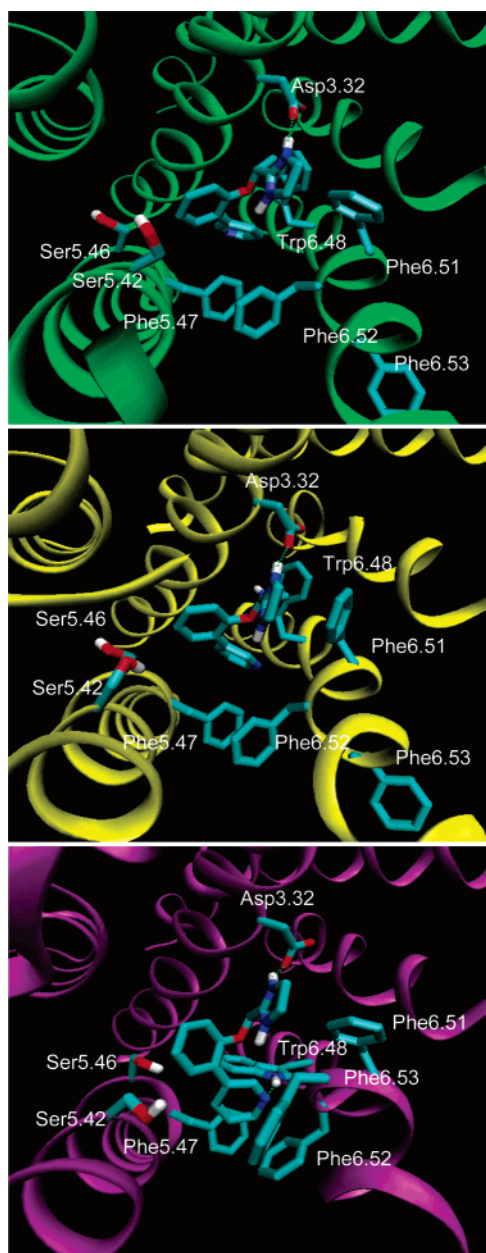
Most modeling studies of aminergic receptors predict that the agonist binding site is located within the water-accessible binding site crevice located within TM3, TM5, TM6, and TM7. Thus our docking studies, to be valuable, should at least fulfill this requirement.

Relation of biologic activity to molecular orientation is simpler when affinity, determined by radioligand binding assays, is used, rather than intrinsic activity. It is quite difficult to model how agonist binding is converted into receptor activation. Nevertheless, the receptor–ligand complexes predicted by our model were able to reproduce some basic interactions that stabilize binding and possibly represent the initial step of the receptor activation process depicted in Figure 3.

First of all, the salt bridge between the highly conserved Asp3.32 and the charged nitrogen of the agonist is observed; it is well-known that the same kind of interaction takes place when natural ligands (i.e., catecholamines) bind to the receptor cavity. It has also been proposed<sup>59,60</sup> that the disruption of an ionic lock, formed by the same aspartate and some negatively charged residues located in TM6 or TM7, is a crucial switch governing receptor activation.

In addition to this, the phenoxy ring of compound **5** is pointing toward TM5, with the carbon atoms in the





**Figure 3.** Compound **5** docked in the receptor binding site (green,  $\alpha_{2A}$ ; yellow,  $\alpha_{2B}$ ; purple,  $\alpha_{2C}$ ). Side chains of the residues interacting with the agonist are displayed to help interpretation.

meta and para positions facing a motif made by a pair of serines common to all the adrenoceptors (Ser5.42 and Ser5.46). As demonstrated by mutagenesis data<sup>61,62</sup> and by previous docking studies performed by some of us,<sup>63</sup> these polar residues interact through a hydrogen-bond network with the catecholic hydroxyls of noradrenaline. In the case of compound **5**, although the same kind of interactions cannot take place, due to the absence of proper substituents on the phenoxy moiety, it is anyway clear that a reliable binding mode is achieved for this highly active agonist. As a consequence of this, portion X (Chart 1) is therefore merged in a broad lipophilic zone made up by Phe6.44, Trp6.48, Phe6.51, Phe6.52, and Phe6.53 (Table 4 and Figure 3). According to the finding of Ballesteros et al.,<sup>64</sup> in this zone of a GPCR a cluster of highly conserved aromatic residues faces the binding site cavity; when an agonist binds or interacts

**Table 5.** Binding Energy for Compound **5** As Determined by the Docking Studies

receptor	estimated $pI$	free energy (kcal/mol)	H bond (kcal/mol)
$\alpha_{2A}$	5.4	-7.34	-0.96
$\alpha_{2B}$	5.6	-7.65	-1.22
$\alpha_{2C}$	6.5	-8.84	-1.60

with some residues of this aromatic cluster, some structural arrangements might occur that in turn would lead to receptor activation. It can be observed above that all  $\alpha_{2C}$ , but also  $\alpha_{2A}$ , subtypes present a more puckered aromatic cluster with respect to the  $\alpha_{2B}$ -subtype; probably this means that  $\pi$ - $\pi$  aromatic stacking between portion X (provided that its chemical nature allows this) and side chains of Phe6.51, Phe6.52, and Phe6.53 takes place, to a large extent determining efficient  $\alpha_{2A}$ - and  $\alpha_{2C}$ -agonism (for example, compounds **3**, **7**, and **8**).

Very interestingly, in the same zone the docking of compound **5** to the three  $\alpha_2$ -AR subtypes shows the most significant differences, giving some valuable clues that might help interpretation of the observed selectivity of this compound. In fact, the most interesting observation regards the interaction between the pyridine nitrogen in position 3 of **5** and the NH-indole ring of Trp6.48, the latter being differently oriented in the three receptor-ligand complexes; while in the case of  $\alpha_{2A}$  and  $\alpha_{2B}$  this residue is pointing toward TM2, in that of  $\alpha_{2C}$  it is interacting strongly with the ligand by means of a hydrogen bond that is not present when the same agonist binds to the other two subtypes. This evidence is also supported by the free energy of binding and the hydrogen-bond contribution, as measured by the Flo+ scoring function (Table 5). The same kind of interaction can be hypothesized for OH, NO<sub>2</sub>, and F substituents in the meta position of other  $\alpha_{2C}$ -selective agonists, **13**, **16**, and **19**, respectively.

According to our findings, a possible explanation for the  $\alpha_{2C}$  selectivity of compound **5** might be given. Since the residues comprising the binding cavity are highly conserved in all three receptor subtypes, a difference in terms of accessibility and/or shape (mainly close to the aromatic cluster controlling the activation process) might be responsible for the observed selectivity. This is also confirmed by the nature of the extracytoplasmic end of TM6, which in our model is a right-handed  $\alpha$ -helix for  $\alpha_{2A}$ - and  $\alpha_{2B}$ - but a left-handed one in the case of  $\alpha_{2C}$ -AR subtypes.

Although our models need better refinement, it is worth noting that some structural features, able to justify the differences in terms of efficacy among the three  $\alpha_2$ -AR subtypes, have been properly identified and highlighted. This study also supports the hypothesis that the possible interactions of portion X of the above agonists with a residue or residues in the TM6 aromatic cluster might be the initiating event leading to activation of the GPCRs. For this purpose, and to gain more insight into this very interesting biological process, exhaustive molecular dynamics simulation on the ligand-receptor complexes is already being planned.

## Conclusion

From the results of the present study, it emerges that among the ligands bearing the basic structure of 4,5-

dihydro-2-(1-phenoxyethyl)-1*H*-imidazole, the aromatic nature of the portion X (Chart 1) is important for activating the  $\alpha_{2A}$ - and  $\alpha_{2C}$ -AR subtypes (compounds **3**, **7**, and **8**). The incompatible steric hindrance and/or the decrease in aromaticity resulting from the introduction of deactivating chemical functions significantly weaken the efficacy of the interactions to the point of producing compounds that are totally devoid of adrenergic activity. However, a correct spatial orientation of the dipole originated by such functions (pyridine nitrogen in position 3 of **5** and OH, NO<sub>2</sub>, and F in the meta position of **13**, **16**, and **19**, respectively), allowing the formation of a hydrogen bond with a corresponding receptor function, results in efficient and selective activation of the  $\alpha_{2C}$ -AR subtype. Modeling studies support the experimental data and highlight this bond between the pyridine nitrogen in position 3 of **5** and the NH-indole ring of Trp6.48, which is favorably oriented in the  $\alpha_{2C}$ -subtype, only.

In conclusion, we have confirmed that it is possible, by conservative structural modifications, to modulate the selectivity profile of ligands inside a receptor system. The imidazoline derivatives **5**, **13**, **16**, and **19**, which exhibit significant selectivity for the  $\alpha_{2C}$ -AR subtype, constitute an important basis for future work and may be useful for characterizing functions specifically governed by this subtype.

### Experimental Protocols

**Chemistry.** Melting points were taken in glass capillary tubes on a Buchi SMP-20 apparatus and are uncorrected. IR and NMR spectra were recorded on Perkin-Elmer 297 and Varian EM-390 instruments, respectively. Chemical shifts are reported in parts per million (ppm) relative to tetramethylsilane (TMS), and spin multiplicities are given as s (singlet), d (doublet), t (triplet), q (quartet), or m (multiplet). IR spectral data (not shown because of the lack of unusual features) were obtained for all compounds reported and are consistent with the assigned structures. The microanalyses were performed by the Microanalytical Laboratory of our department. The elemental composition of the compounds agreed to within  $\pm 0.4\%$  of the calculated value. Chromatographic separations were performed on silica gel columns (Kieselgel 40, 0.040–0.063 mm, Merck) by flash chromatography. The term “dried” refers to the use of anhydrous sodium sulfate. Compounds were named following IUPAC rules as applied by Beilstein-Institut AutoNom (version 2.1), software for systematically naming organic chemicals.

**Preparation of imidazolines 4–23 and bioisosters 24–26.** **Method A.** 2'-[2-[1-(4,5-Dihydro-1*H*-imidazol-2-yl)ethoxy]phenyl]pyridine (**4**). A mixture of **27** (0.67 g, 3.0 mmol), sodium methoxide (0.014 g, 0.26 mmol), and MeOH (2 mL) was stirred for 18 h. On cooling to 0–10 °C, a solution of ethylenediamine (0.22 mL, 3.36 mmol) in MeOH (1 mL) was added dropwise with stirring; after a few minutes a solution of HCl in MeOH (1.043 mL of 3 N solution, 3.13 mmol) was added dropwise and the mixture was allowed to warm to room temperature. After 78 h, the mixture was made slightly acid with methanolic HCl and filtered. The filtrate was evaporated and the residue was taken up in H<sub>2</sub>O. The solution was basified with 2 N NaOH and extracted with CHCl<sub>3</sub>. The organic layer was dried over Na<sub>2</sub>SO<sub>4</sub> and evaporated to give a residue that was purified by flash chromatography (Table 6). The free base was transformed into the oxalate salt, whose physicochemical properties are reported in Table 6.

Similarly, compounds **5–7**, **9–12**, **16**, and **21–23** (Table 6) were obtained from the suitable nitriles.

**Method B.** 2'-[1-(4,5-Dihydro-1*H*-imidazol-2-yl)ethoxy]biphenyl-3-ylamine (**18**). Compound (**18**) (0.1 g, 0.32 mmol) was hydrogenated in MeOH for 6 h at room temperature under

pressure (45 psi) using Pd/C as catalyst. Following catalyst removal, the evaporation of the solvent gave the free base that was transformed into the oxalate salt (Table 6).

**Method C.** 2'-[1-(4,5-Dihydro-1*H*-imidazol-2-yl)ethoxy]biphenyl-4-ol (**14**). HCl was bubbled through a stirred and cooled (0 °C) solution of **40** (0.69 g, 2.88 mmol) and MeOH (0.24 mL, 5.76 mmol) in dry CHCl<sub>3</sub> (5 mL) for 45 min. After 12 h at 0 °C, dry ether was added to the reaction mixture to give the intermediate imidate, which was filtered. This solid (0.154 g, 0.50 mmol) was added to a cooled (0 °C) and stirred solution of ethylenediamine (0.041 mL, 0.62 mmol) in absolute EtOH (2.4 mL). After 1 h, concentrated HCl (a few drops) in absolute EtOH (1.2 mL) was added to the reaction mixture, which was stored overnight in the refrigerator. It was then diluted with absolute EtOH (2 mL) and heated at 75 °C for 5 h. After cooling, the solid was collected and discarded, and the filtrate was concentrated and filtered again. The filtrate was evaporated to dryness to give a residue, which was taken up in CHCl<sub>3</sub> (20 mL), washed with 2 N NaOH, and dried over Na<sub>2</sub>SO<sub>4</sub>. Removal of the solvent gave a residue that was purified by flash chromatography and then transformed into the hydrochloride salt (Table 6).

**Method D.** 2-[1-(3'-Fluorobiphenyl-2-yloxy)ethyl]-4,5-dihydro-1*H*-imidazole (**19**). A mixture of ethylenediamine (3.4 mL) and **42** (1.2 g, 4.97 mmol) was heated at 115 °C for 6 h. After cooling and addition of H<sub>2</sub>O, the mixture was extracted with CHCl<sub>3</sub>. The organic layer was washed with H<sub>2</sub>O, dried over Na<sub>2</sub>SO<sub>4</sub>, and evaporated to give a residue that was purified by flash chromatography and then transformed into the oxalate salt (Table 6).

Similarly, compounds **15** and **17** (Table 6) were obtained from the suitable nitriles.

**Method E.** 2'-[1-(4,5-Dihydro-1*H*-imidazol-2-yl)ethoxy]biphenyl-3-ol (**13**). A mixture of 2-aminoethylammonium toluene-*p*-sulfonate (11.38 g, 49 mmol) and **39** (1.17 g, 4.9 mmol) was heated at 200 °C for 2 h. After cooling and addition of H<sub>2</sub>O, the solution was extracted with CHCl<sub>3</sub>. The organic layer was washed with H<sub>2</sub>O, dried over Na<sub>2</sub>SO<sub>4</sub>, and evaporated to give a residue that was purified by flash chromatography and transformed into the oxalate salt (Table 6).

**Method F.** 2-[1-(2-Thiophen-3-ylphenoxy)ethyl]-4,5-dihydro-1*H*-imidazole (**8**). A solution of ethylenediamine (1.29 mL, 19.30 mmol) in dry toluene (6.7 mL) was added dropwise to a mechanically stirred solution of 2 M trimethylaluminum (9.6 mL, 19.30 mmol) in dry toluene (16 mL) at 0 °C in nitrogen atmosphere. After being stirred at room temperature for 1 h, the solution was cooled to 0 °C and a solution of **46** (2.54 g; 9.64 mmol) in dry toluene (11.5 mL) was added dropwise. The reaction mixture was heated to 110 °C for 3 h, cooled to 0 °C, and quenched cautiously with MeOH (4.5 mL) followed by H<sub>2</sub>O (1 mL). After addition of CHCl<sub>3</sub> (35 mL), the mixture was left for 30 min at room temperature to ensure the precipitation of the aluminum salts. The mixture was filtered and the organic layer was extracted with 2 N HCl. The aqueous layer was made basic with 10% NaOH and extracted with CHCl<sub>3</sub>. The organic layer was dried over Na<sub>2</sub>SO<sub>4</sub>, filtered, and evaporated to give the free base, which was purified by flash chromatography and then transformed into the oxalate salt (Table 6).

**Method G.** 5-[1-(Biphenyl-2-yloxy)ethyl]-3,4-dihydro-2*H*-pyrrole (**26**). Sodium hydride (0.66 g of a 50% dispersion in mineral oil, 13.73 mmol) contained in a 100 mL flask was washed with three 5-mL portions of hexane. The flask was fitted with a reflux condenser, flushed with nitrogen, and charged with 20 mL of dry THF. A solution of 2-(biphenyl-2-yloxy)propionic acid methyl ester<sup>36</sup> (2.64 g, 10.3 mmol) and *N*-vinylpyrrolidinone (1.27 g, 11.4 mmol) in 3 mL of dry THF was added in one portion. The mixture was stirred and, after several minutes, an exothermic reaction with gas evolution started. When the evolution of gas had ceased, the mixture was heated under reflux for 1 h and then cooled to room temperature. Concentrated HCl (1.72 mL), diluted with 5.72 mL of H<sub>2</sub>O, was added, and the mixture was heated under reflux overnight. After cooling, the solution was made basic by the addition of concentrated aqueous NaOH (ice bath cooling). The



**Table 6.** Physicochemical Properties of Oxalate, Sulfate, and Hydrochloride Salts of Imidazolines 4–26

compd	eluent composition <sup>a</sup>	yield, %	mp, °C (recryst solvent)	<sup>1</sup> H NMR (DMSO), $\delta$
4	5:4:1:0.1	40	152–155 (dry EtOH)	1.57 (d, 3, CH <sub>3</sub> ), 3.92 (s, 4, NCH <sub>2</sub> CH <sub>2</sub> N), 5.55 (q, 1, CH), 7.18–8.72 (m, 8, ArH)
5	5:4:1:0.1	37	160–163 (dry EtOH)	1.52 (d, 3, CH <sub>3</sub> ), 3.86 (s, 4, NCH <sub>2</sub> CH <sub>2</sub> N), 5.35 (q, 1, CH), 7.08–8.80 (m, 8, ArH), 12.00 (br s, 1, NH, exchangeable with D <sub>2</sub> O)
6	5:4:1:0.1	38	143–145 (dry EtOH)	1.50 (d, 3, CH <sub>3</sub> ), 3.86 (s, 4, NCH <sub>2</sub> CH <sub>2</sub> N), 5.34 (q, 1, CH), 7.05–8.63 (m, 8, ArH), 10.52 (br s, 1, NH, exchangeable with D <sub>2</sub> O)
7	5:3:2:0.1	36	155–158 (i-PrOH/Et <sub>2</sub> O)	1.62 (d, 3, CH <sub>3</sub> ), 3.90 (s, 4, NCH <sub>2</sub> CH <sub>2</sub> N), 5.48 (q, 1, CH), 7.03–7.80 (m, 7, ArH)
8	5:3:2:0.1	40	168–169 (i-PrOH)	1.56 (d, 3, CH <sub>3</sub> ), 3.86 (s, 4, NCH <sub>2</sub> CH <sub>2</sub> N), 5.31 (q, 1, CH), 7.02–7.87 (m, 7, ArH)
9 <sup>b</sup>	6:4:1:0.1	31	158–159 (i-PrOH)	1.30 (d, 3, CH <sub>3</sub> ), 2.12 (s, 3, Ph-CH <sub>3</sub> ), 3.82 (s, 4, NCH <sub>2</sub> CH <sub>2</sub> N), 4.96 (q, 1, CH), 7.10–7.42 (m, 8, ArH), 10.06 (br s, 1, NH, exchangeable with D <sub>2</sub> O)
10	6:4:1:0.1	41	160–161 (i-PrOH)	1.45 (d, 3, CH <sub>3</sub> ), 2.38 (s, 3, Ph-CH <sub>3</sub> ), 3.83 (s, 4, NCH <sub>2</sub> CH <sub>2</sub> N), 5.17 (q, 1, CH), 7.03–7.40 (m, 8, ArH)
11	6:4:1:0.1	42	187–188 (i-PrOH)	1.47 (d, 3, CH <sub>3</sub> ), 2.38 (s, 3, Ph-CH <sub>3</sub> ), 3.85 (s, 4, NCH <sub>2</sub> CH <sub>2</sub> N), 5.20 (q, 1, CH), 7.00–7.50 (m, 8, ArH)
12	5:4:2:0.1	30	180 (i-PrOH/dry EtOH)	1.43 (d, 3, CH <sub>3</sub> ), 3.85 (m, 4, NCH <sub>2</sub> CH <sub>2</sub> N), 5.17 (q, 1, CH), 6.82–7.38 (m, 8, ArH), 10.18 (br s, 1, NH, exchangeable with D <sub>2</sub> O)
13	3:7:1:0.1	60	101–102 (i-PrOH)	1.43 (d, 3, CH <sub>3</sub> ), 3.82 (s, 4, NCH <sub>2</sub> CH <sub>2</sub> N), 5.05 (q, 1, CH), 6.72–7.45 (m, 8, ArH), 7.68 (br s, 1, OH, exchangeable with D <sub>2</sub> O), 10.17 (br s, 1, NH, exchangeable with D <sub>2</sub> O)
14 <sup>c</sup>	6:4:1:0.1	85	240 (i-PrOH)	1.43 (d, 3, CH <sub>3</sub> ), 3.83 (s, 4, NCH <sub>2</sub> CH <sub>2</sub> N), 5.10 (q, 1, CH), 6.80–7.41 (m, 8, ArH), 9.58 (s, 1, OH, exchangeable with D <sub>2</sub> O), 10.35 (br s, 1, NH, exchangeable with D <sub>2</sub> O)
15 <sup>c</sup>	7:3:1:0.1	35	235 (dry EtOH)	1.32 (d, 3, CH <sub>3</sub> ), 3.80 (s, 4, NCH <sub>2</sub> CH <sub>2</sub> N), 5.18 (q, 1, CH), 7.02–8.08 (m, 8, ArH), 10.25 (br s, 1, NH, exchangeable with D <sub>2</sub> O)
16	4:6:1:0.1	33	208–210 (dry EtOH)	1.53 (d, 3, CH <sub>3</sub> ), 3.88 (s, 4, NCH <sub>2</sub> CH <sub>2</sub> N), 3.93 (br s, 1, NH, exchangeable with D <sub>2</sub> O), 5.38 (q, 1, CH), 7.08–7.47 (m, 8, ArH)
17	7:3:1:0.1	40	206–208 (dry EtOH)	1.48 (d, 3, CH <sub>3</sub> ), 3.85 (s, 4, NCH <sub>2</sub> CH <sub>2</sub> N), 4.25 (br s, 1, NH, exchangeable with D <sub>2</sub> O), 5.32 (q, 1, CH), 7.03–8.33 (m, 8, ArH)
18	—	99	158–160 (dry EtOH)	1.51 (d, 3, CH <sub>3</sub> ), 3.83 (s, 4, NCH <sub>2</sub> CH <sub>2</sub> N), 5.10 (q, 1, CH), 6.55–7.37 (m, 8, ArH), 8.92 (br s, 2, exchangeable with D <sub>2</sub> O), 10.5 (br s, 1, NH, exchangeable with D <sub>2</sub> O)
19	5:5:1:0.1	74	102–103 (i-PrOH/Et <sub>2</sub> O)	1.48 (d, 3, CH <sub>3</sub> ), 3.87 (s, 4, NCH <sub>2</sub> CH <sub>2</sub> N), 5.27 (q, 1, CH), 7.03–7.52 (m, 8, ArH)
21	6:4:1:0.1	40	169–170 (i-PrOH)	1.38 (d, 3, CH <sub>3</sub> ), 3.66 (s, 4, NCH <sub>2</sub> CH <sub>2</sub> N), 4.14 (q, 1, CH), 7.27–7.62 (m, 9, ArH), 10.06 (br s, 1, NH, exchangeable with D <sub>2</sub> O)
22	6:4:1:0.1	50	165–167 (dry EtOH)	3.66 (m, 4, NCH <sub>2</sub> CH <sub>2</sub> N), 4.10 (br s, 1, NH, exchangeable with D <sub>2</sub> O), 4.32 (d, 1, CH=C=N), 4.43 (d, 1, ArCH), 7.35–7.55 (m, 9, ArH)
23	6:4:1:0.1	60	158–160 (dry EtOH)	3.84 (s, 4, NCH <sub>2</sub> CH <sub>2</sub> N), 4.04 (d, 1, CH=CdN), 4.15 (br s, 1, NH, exchangeable with D <sub>2</sub> O), 4.27 (d, 1, ArCH), 7.30–7.55 (m, 9, ArH)
24 <sup>d</sup>	7:3 <sup>e</sup>	25	87–90	1.52 (d, 3, CH <sub>3</sub> ), 3.87 (t, 2, NCH <sub>2</sub> CH <sub>2</sub> O), 4.25 (m, 2, NCH <sub>2</sub> CH <sub>2</sub> O), 4.93 (q, 1, CH), 7.03–7.65 (m, 9, ArH)
25 <sup>c</sup>	8:2 <sup>e</sup>	20	104–105 (i-PrOH/Et <sub>2</sub> O)	1.42 (d, 3, CH <sub>3</sub> ), 3.28 (m, 2, SCH <sub>2</sub> CH <sub>2</sub> N), 4.22 (t, 2, SCH <sub>2</sub> CH <sub>2</sub> N), 4.78 (br s, 1, NH, exchangeable with D <sub>2</sub> O), 5.30 (q, 1, CH), 7.03–7.60 (m, 9, ArH)
26	5:5 <sup>e</sup>	58	94–95 (i-PrOH)	1.38 (d, 3, CH <sub>3</sub> ), 1.72 (m, 2, NCH <sub>2</sub> CH <sub>2</sub> CH <sub>2</sub> ), 2.30 (m, 2, NCH <sub>2</sub> CH <sub>2</sub> CH <sub>2</sub> ), 3.73 (m, 2, NCH <sub>2</sub> CH <sub>2</sub> CH <sub>2</sub> ), 5.18 (q, 1, CH), 7.02–7.78 (m, 9, ArH)

<sup>a</sup> For flash chromatography cyclohexane/AcOEt/MeOH/33% NH<sub>4</sub>OH was eluent for the free base. <sup>b</sup> Sulfate salt. <sup>c</sup> Hydrochloride salt. <sup>d</sup> Free base. <sup>e</sup> Cyclohexane/AcOEt was eluent for the free base.

precipitated product was extracted with CH<sub>2</sub>Cl<sub>2</sub>. The pooled extracts were washed with H<sub>2</sub>O, dried over Na<sub>2</sub>SO<sub>4</sub>, and evaporated. The crude product was purified by flash chromatography and transformed into the oxalate salt (Table 6).

**Method H. 2-[1-(Biphenyl-2-yloxy)ethyl]-4,5-dihydrothiazole (25).** A stirred solution of 2-(biphenyl-2-yloxy)propionic acid<sup>41</sup> (2.15 g, 8.89 mmol), 2-aminoethanethiol (0.683 g, 8.89 mmol), triphenylphosphine (6.97 g, 26.57 mmol), triethylamine (2.7 g, 26.57 mmol), and CCl<sub>4</sub> (13.8 g, 88.9 mmol) in CH<sub>3</sub>CN (30 mL) was heated at 40 °C for 4 h. The solvent was removed under reduced pressure to give a residue that was taken up in AcOEt. The insoluble solid was filtered and washed with AcOEt. The solvent was evaporated and the residue was purified by flash chromatography and transformed into the hydrochloride salt (Table 6).

**Method I. 2-[1-(Biphenyl-2-yloxy)ethyl]-4,5-dihydrooxazole (24).** 2-(Biphenyl-2-yloxy)propionic acid<sup>41</sup> (2.78 g, 11.47 mmol) was dissolved in dry CH<sub>2</sub>Cl<sub>2</sub> under nitrogen atmosphere. After addition of oxalyl chloride (1.51 mL, 16.6 mmol) the mixture was stirred at room temperature for 2 days. Excess oxalyl chloride was removed in vacuo. The reaction flask containing the residue was charged with Et<sub>3</sub>N (1.96 mL, 14.04 mmol), 2-aminoethanol (1.51 mL, 24.6 mmol), and dry CH<sub>2</sub>Cl<sub>2</sub> (45 mL). The mixture was stirred overnight, quenched with saturated aqueous NH<sub>4</sub>Cl solution (15 mL) and H<sub>2</sub>O (15 mL), and then extracted with Et<sub>2</sub>O. The organic layer was washed with H<sub>2</sub>O, dried over Na<sub>2</sub>SO<sub>4</sub>, and evaporated. The residue was dissolved in dry CH<sub>2</sub>Cl<sub>2</sub> (180 mL), cooled to 0 °C, treated with SOCl<sub>2</sub> (3.77 mL, 51.3 mmol), and stirred at room temperature for 24 h. After removal of the excess SOCl<sub>2</sub> by evaporation,

the residue was dissolved in CH<sub>2</sub>Cl<sub>2</sub> and washed with brine. The organic layer was dried over Na<sub>2</sub>SO<sub>4</sub> and evaporated. Et<sub>3</sub>N (15.1 mL, 108.7 mmol) and CHCl<sub>3</sub> (75 mL) were added, and the mixture was refluxed for 3 days, extracted with cold H<sub>2</sub>O, dried over Na<sub>2</sub>SO<sub>4</sub>, filtered, and evaporated. The product was purified by flash chromatography to give the free base **24** (Table 6).

**Preparation of nitriles 27–44. Method A. 2-(2-Pyridin-2-ylphenoxy)propionitrile (27).** A mixture of 2-pyridin-2-ylphenol<sup>42</sup> (0.33 g, 1.93 mmol), 2-chloropropionitrile (0.173 g, 1.93 mmol), and K<sub>2</sub>CO<sub>3</sub> (0.27 g, 1.93 mmol) in DME was refluxed for 8 h. The mixture was cooled and filtered. The solvent was removed under reduced pressure to give a residue, which was taken up in AcOEt and washed with cold 2 N NaOH. Removal of dried solvent afforded an oil whose physicochemical properties are reported in Table 7.

Similarly, compounds **28**, **29**, and **30** were obtained from 4-pyridin-4-ylphenol,<sup>42</sup> 2'-nitrobiphenyl-2-ol,<sup>43b</sup> and 4'-nitrobiphenyl-2-ol,<sup>43a</sup> respectively. Compound **44** was generated from 2-bromobenzenethiol (Table 7).

**Method B. trans- and cis-3-Biphenyl-2-yloxirane-2-carbonitrile (31 and 32).** A solution of potassium *tert*-butoxide (0.743 g, 6.62 mmol) in dry *tert*-butyl alcohol (6.5 mL) was added dropwise to a solution of 2-biphenylcarboxaldehyde (1.18 g, 6.47 mmol) and chloroacetonitrile (0.48 g, 6.47 mmol) with stirring and cooling under nitrogen atmosphere. The reaction was allowed until TLC indicated the absence of 2-biphenylcarboxaldehyde. *tert*-Butyl alcohol was removed in vacuo and H<sub>2</sub>O (6 mL) was added to the residue. Extraction with ether, drying over Na<sub>2</sub>SO<sub>4</sub>, and removal of the solvent in

**Table 7.** Physicochemical Properties of Nitriles 27–44

compd	eluent composition <sup>a</sup>	yield, %	<sup>1</sup> H NMR (CDCl <sub>3</sub> ), $\delta$
27	—	95	1.62 (d, 3, CH <sub>3</sub> ), 4.81 (q, 1, CH), 7.17–8.67 (m, 8, ArH)
28	—	94	1.68 (d, 3, CH <sub>3</sub> ), 4.81 (q, 1, CH), 7.18–8.65 (m, 8, ArH)
29	5:5 <sup>b</sup>	85	1.58 (d, 3, CH <sub>3</sub> ), 4.82 (q, 1, CH), 7.08–8.03 (m, 8, ArH)
30	8:2 <sup>b</sup>	93	1.70 (d, 3, CH <sub>3</sub> ), 4.83 (q, 1, CH), 7.08–8.33 (m, 8, ArH)
31	10:0.5	59	3.40 (d, 1, <i>J</i> = 1.83 Hz, CHCN), 4.22 (d, 1, <i>J</i> = 1.83 Hz, ArCH), 7.18–7.52 (m, 9, ArH)
32	10:0.5	32	3.66 (d, 1, <i>J</i> = 3.66 Hz, CHCN), 4.11 (d, 1, <i>J</i> = 3.66 Hz, ArCH), 7.30–7.48 (m, 9, ArH)
33	8.5:1.5	68	1.62 (d, 3, CH <sub>3</sub> ), 4.80 (q, 1, CH), 7.15–8.78 (m, 8, ArH)
34	9.5:0.5	46	1.87 (d, 3, CH <sub>3</sub> ), 4.92 (q, 1, CH), 7.10–7.70 (m, 8, ArH)
35	9.5:0.5	95	1.48 (d, 3, CH <sub>3</sub> ), 2.18 (s, 3, ArCH <sub>3</sub> ), 4.58 (q, 1, CH), 7.17–7.47 (m, 8, ArH)
36	9.5:0.5	95	1.62 (d, 3, CH <sub>3</sub> ), 2.43 (s, 3, ArCH <sub>3</sub> ), 4.62 (q, 1, CH), 7.18–7.42 (m, 8, ArH)
37	9.5:0.5	92	1.65 (d, 3, CH <sub>3</sub> ), 2.45 (s, 3, ArCH <sub>3</sub> ), 4.63 (q, 1, CH), 7.20–7.66 (m, 8, ArH)
38	8:2	50	1.62 (d, 3, CH <sub>3</sub> ), 4.63 (q, 1, CH), 4.60 (br, 1, OH, exchangeable with D <sub>2</sub> O), 7.00–7.54 (m, 8, ArH)
39	8:2	52	1.62 (d, 3, CH <sub>3</sub> ), 4.63 (q, 1, CH), 6.82–7.40 (m, 8, ArH)
40	8:2	51	1.62 (d, 3, CH <sub>3</sub> ), 4.63 (q, 1, CH), 5.40 (br s, 1, OH, exchangeable with D <sub>2</sub> O), 6.83–7.45 (m, 8, ArH)
41	8:2	92	1.72 (d, 3, CH <sub>3</sub> ), 4.83 (q, 1, CH), 7.20–8.43 (m, 8, ArH)
42	6:4 <sup>b</sup>	90	1.64 (d, 3, CH <sub>3</sub> ), 4.71 (q, 1, CH), 7.02–7.45 (m, 8, ArH)
43	—	53	1.72 (d, 3, CH <sub>3</sub> ), 4.30 (q, 1, CH), 7.22–7.73 (m, 4, ArH)
44	9:1	58	1.42 (d, 3, CH <sub>3</sub> ), 3.53 (q, 1, CH), 7.36–7.75 (m, 9, ArH)

<sup>a</sup> For flash chromatography. Cyclohexane/AcOEt. <sup>b</sup> For flash chromatography. Cyclohexane/CH<sub>2</sub>Cl<sub>2</sub>.

vacuo gave a residue; from this, stereoisomers **31** (first fraction) and **32** (second fraction) were obtained by flash chromatography (Table 7).

**Method C. 2-(2-Thiophen-2-ylphenoxy)propionitrile (34).** Na<sub>2</sub>CO<sub>3</sub> (1.13 g, 10.7 mmol), H<sub>2</sub>O (5.35 mL), and tetrakis-(triphenylphosphine)palladium(0) (0.255 g, 0.221 mmol) were added to a solution of 2-(2-bromophenoxy)propionitrile (1 g, 4.42 mmol) and 2-thiophenboronic acid (0.7 g, 5.52 mmol) in DME (8 mL). The mixture was heated at 90 °C for 14 h in the dark under nitrogen atmosphere. Then it was cooled to room temperature and poured into AcOEt and ice. The organic layer was separated, washed with H<sub>2</sub>O, dried over Na<sub>2</sub>SO<sub>4</sub>, and evaporated. The residue was purified by flash chromatography (Table 7).

Similarly, compounds **33** and **35–42** were obtained from the suitable boronic acids. Compound **43** was generated by treating 2-(2-bromophenylsulfanyl)propionitrile (**44**) with phenyl boronic acid (Table 7).

**2-(2-Thiophen-3-ylphenoxy)propionic Acid Methyl Ester (46).** A mixture of 2-bromophenol (1.41 g, 8.15 mmol), methyl 2-bromopropionate (1.36 g, 8.15 mmol), and K<sub>2</sub>CO<sub>3</sub> (1.13 g, 8.15 mmol) in DME was refluxed for 8 h. The mixture was cooled and filtered. The solvent was removed under reduced pressure, and the remaining residue was taken up in AcOEt and washed with cold 2 N NaOH. Removal of dried solvent afforded an oil, which was purified by flash chromatography using cyclohexane/AcOEt (95:5) as eluent, to give 1.9 g (yield 90%) of 2-(2-bromophenoxy)propionic acid methyl ester (**45**): <sup>1</sup>H NMR (CDCl<sub>3</sub>)  $\delta$  1.72 (d, 3, CH<sub>3</sub>), 3.78 (s, 3, COOCH<sub>3</sub>), 4.88 (q, 1, CH), 6.80–7.61 (m, 4, ArH).

Na<sub>2</sub>CO<sub>3</sub> (1.13 g, 10.7 mmol), H<sub>2</sub>O (5.35 mL), and tetrakis-(triphenylphosphine)palladium(0) (0.255 g, 0.221 mmol) were added to a solution of **45** (1.15 g, 4.42 mmol) and 3-thiophenboronic acid (0.7 g, 5.52 mmol) in DME (8 mL). The mixture was heated at 90 °C for 14 h in the dark under nitrogen atmosphere. After cooling to room temperature the mixture was poured into AcOEt and ice and extracted with CHCl<sub>3</sub>. The organic layer was dried over Na<sub>2</sub>SO<sub>4</sub>, filtered, and evaporated in vacuo to give the corresponding acid which was converted into the methyl ester by heating in CH<sub>3</sub>OH in the presence of a catalytic amount of H<sub>2</sub>SO<sub>4</sub>. After cooling, the solvent was evaporated to dryness to give a residue which was taken up in CHCl<sub>3</sub> and washed with NaHCO<sub>3</sub> and H<sub>2</sub>O. The organic layer was dried over Na<sub>2</sub>SO<sub>4</sub> and evaporated to give a residue that was purified by flash chromatography using cyclohexane/AcOEt (95:5) as eluent. Compound **46** was obtained as an oil (0.92 g; yield 46%): <sup>1</sup>H NMR (CDCl<sub>3</sub>)  $\delta$  1.63 (d, 3, CH<sub>3</sub>), 3.78 (s, 3, COOCH<sub>3</sub>), 4.82 (q, 1, CH), 6.80–7.75 (m, 7, ArH).

**Generation of CHO Clones Expressing  $\alpha_2$ -AR Subtypes.** CHO cells were routinely subcultured in Dulbecco's Modified Eagle's Medium (DMEM) supplemented with

5% fetal calf serum. The plasmids used to express  $\alpha_{2A}$ - ( $\alpha_2C10Eneo$ ),  $\alpha_{2B}$ - ( $\alpha_2C2Eneo$ ), or  $\alpha_{2C}$ -AR ( $\alpha_2C4Eneo$ ) had been described earlier.<sup>65</sup> Briefly, each bicistronic vector contains an expression cassette comprising the human cytomegalovirus early promoter/enhancer, the entire ORF encoding for  $\alpha_{2A}$ -,  $\alpha_{2B}$ - or  $\alpha_{2C}$ -AR, an internal ribosome entry site derived from encephalomyocarditis virus, the neomycin phosphotransferase gene, and a rabbit  $\beta$ -globin genomic sequence containing an intron and a polyadenylation signal. CHO cells were transfected using the calcium-phosphate method. At 2 days post-transfection, cells were subcultured in the presence of G418-sulfate (1 mg/mL) and antibiotic resistant clones were collected individually using cloning cylinders.

**Binding Experiments.** Binding experiments were carried out on crude membrane preparations using the selective radioligand [<sup>3</sup>H]RX821002 ( $\alpha_2$ -antagonist). Frozen cell pellets were homogenized in 5 mL of Tris-Mg buffer (50 mM Tris-HCl, 0.5 mM MgCl<sub>2</sub>, pH 7.5) and centrifuged at 39 000g for 10 min. The particulate fraction was washed, the final crude membrane pellet was taken up in the appropriate volume of Tris-Mg buffer, and the protein concentration was determined using the Coomassie Blue method.<sup>66</sup> Total binding was measured by incubating 100  $\mu$ L of cell membrane preparation with the radioligand in a total volume of 400  $\mu$ L of TM buffer. After a 30-min period of incubation at 25 °C, bound radioligand was separated from free by filtration through GF/C Whatman filters using a Skatron cell harvester (Skatron, Lier, Norway). Filters were rapidly washed with ice-cold buffer, and radioactivity was determined by liquid scintillation spectrometry. Specific binding was defined as the difference between total and nonspecific binding measured in the presence of 10<sup>-4</sup> M phentolamine. For saturation studies, the final concentrations of [<sup>3</sup>H]RX821002 ranged from 0.1 to 15 nM. Inhibition experiments were carried out at a fixed concentration of radioligand corresponding to twice its *K*<sub>d</sub> value for the considered subtype (2 nM for  $\alpha_{2A}$ -AR, 8 nM for  $\alpha_{2B}$ -AR, and 4 nM for  $\alpha_{2C}$ -AR). Competition curves were drawn using 12 different concentrations of competitor ranging from 10<sup>-11</sup> to 10<sup>-4</sup> M.

**Functional Assays. Cytosensor Microphysiometry.** Extracellular acidification was measured using an eight-channel cytosensor microphysiometry instrument (Molecular Devices, Menlo Park, CA). Permanent clones of CHO cells expressing human  $\alpha_2$ -ARs individually were seeded into 12 mm capsule cups at a density of 3  $\times$  10<sup>5</sup> cells/cup and incubated at 37 °C under 5% CO<sub>2</sub> atmosphere for 24 h. The capsule cups were loaded into the sensor chambers of the instrument and perfused with a running medium (bicarbonate-free DMEM containing 0.584 g/L glutamine and 2.59 g/L NaCl) at a flow rate of 100  $\mu$ L/min. Agonists were diluted into running medium and injected through a second fluid path. Valves directed the flow from either fluid path to the sensor chamber. For each



90 s pump cycle, the pump was on for 60 s and was then switched off for the remaining 30 s. The pH value was recorded for 20 s (from second 68 to 88). Cells were exposed to agonists for 240 min and consecutive agonist exposures were separated by a 1740-min washing period. This stimulation protocol was validated in preliminary experiments with four known agonists, (–)-noradrenaline, clonidine, UK 14304, and BHT 920. The rate of acidification of the chamber was calculated by the Cytosoft program (Molecular Devices). Changes in the rate of acidification were calculated as the difference between the maximum effect after agonist addition and the average of three measurements taken prior to agonist addition.

**Statistical Analysis.** The values of  $K_i$  and  $EC_{50}$  and the extent of maximal response ( $E_{max}$ ) were calculated from the computer analysis of binding inhibition data and dose–response curves using the program GraphPad Prism (GraphPad Software, San Diego, CA). The results are expressed as means  $\pm$  SEM of three to six separate experiments.

**Acknowledgment.** We thank the MIUR (Rome), CARIMA Foundation (Macerata), and the University of Camerino for financial support.

**Supporting Information Available:** Analysis of reported compounds. This material is available free of charge via the Internet at <http://pubs.acs.org>.

## References

- (1) For part I, see ref 36.
- (2) Ruffolo, R. R., Jr., Ed.; *Adrenoceptors: Structure, Function and Pharmacology*; Harwood Academic Publisher GmbH: Luxembourg, 1995.
- (3) Hoffman, B. B.; Lefkowitz, R. J. Radioligand Binding Studies of Adrenergic Receptors: New Insights into Molecular and Physiological Regulation. *Annu. Rev. Pharmacol. Toxicol.* **1980**, *20*, 581–608.
- (4) Gerhardt, M. A.; Neubig, R. R. Multiple  $G_i$  Protein Subtypes Regulate a Single Effector Mechanism. *Mol. Pharmacol.* **1991**, *40*, 707–711.
- (5) Eason, M. G.; Kurose, H.; Holt, B. D.; Raymond, J. R.; Liggett, S. B. Simultaneous Coupling of  $\alpha_2$ -Adrenergic Receptors to Two G-Proteins with Opposing Effects. Subtype-Selective Coupling of alpha 2C10, alpha 2C4, and alpha 2C2 Adrenergic Receptors to  $G_i$  and  $G_s$ . *J. Biol. Chem.* **1992**, *267*, 15795–15801.
- (6) Hieble, J. P.; Bondinell, W. E.; Ruffolo, R. R., Jr.  $\alpha$ - and  $\beta$ -Adrenoceptors: From the Gene to the Clinic. 1. Molecular Biology and Adrenoceptor Subclassification. *J. Med. Chem.* **1995**, *38*, 3415–3444.
- (7) (a) Bylund, D. B.; Eikenberg, D. C.; Hieble, J. P.; Langer, S. Z.; Lefkowitz, R. J.; Minneman, K. P.; Molinoff, P. B.; Ruffolo, R. R., Jr.; Trendelenburg, U. International Union of Pharmacology Nomenclature of Adrenoceptors. *Pharmacol. Rev.* **1994**, *46*, 121–136. (b) Hieble, J. P.; Ruffolo, R. R., Jr.; Sulpizio, A. C.; Naselsky, D. P.; Conway, T. M.; Ellis, C.; Swift, A. M.; Ganguly, S.; Bergsma, D. J. Functional Subclassification of  $\alpha_2$ -Adrenoceptors. *Pharmacol. Commun.* **1995**, *6*, 91–97.
- (8) Philipp, M.; Brede, M.; Hein, L. Physiological Significance of  $\alpha_2$ -Adrenergic Receptor Subtype Diversity: One Receptor Is Not Enough. *Am. J. Physiol. Regul. Integr. Comput. Physiol.* **2002**, *283*, R287–R295.
- (9) Beeley, L. J.; Berge, J. M.; Chapman, H.; Hieble, J. P.; Kelly, J.; Naselsky, D. P.; Rockell, C. M.; Young, P. W. Synthesis of a Selective  $\alpha_{2A}$  Adrenoceptor Antagonist, BRL 48962, and its Characterization at Cloned Human  $\alpha$ -Adrenoceptors. *Bioorg. Med. Chem.* **1995**, *3*, 1693–1698.
- (10) Gavin, K. T.; Colgan, M. P.; Moore, D.; Shanik, G.; Docherty, J. R.  $\alpha_{2C}$ -Adrenoceptors Mediate Contractile Responses to Noradrenaline in the Human Saphenous Vein. *Naunyn-Schmiedeberg's Arch. Pharmacol.* **1997**, *355*, 406–411.
- (11) Bylund, D. B.; Ray-Prenger, C.; Murphy, T. J.  $\alpha_{2A}$  and  $\alpha_{2B}$  Adrenergic Receptor Subtypes: Antagonist Binding in Tissues and Cell Lines Containing Only One Subtype. *J. Pharmacol. Exp. Ther.* **1998**, *245*, 600–607.
- (12) Fuder, H.; Selbach, M. Characterization of Sensory Neurotransmission and its Inhibition via  $\alpha_{2B}$ -Adrenoceptors and via non- $\alpha_2$ -Adrenoceptors in Rabbit Iris. *Naunyn-Schmiedeberg's Arch. Pharmacol.* **1993**, *347*, 394–401.
- (13) Joutsamo, T.; Tauber, A. Y.; Salo, H.; Hoffren, A. M.; Wurster, S. Compounds Useful for Treatment or Prevention of Disease Mediated by  $\alpha_{2B}$ -Adrenoceptor. WO 03/008387 A1, 2003; *Chem. Abstr.* **2003**, *138*, 122655.
- (14) Uhlen, S.; Lindblom, J.; Johnson, A.; Wikberg, J. E. Autoradiographic Studies of Central  $\alpha_{2A}$ - and  $\alpha_{2C}$ -Adrenoceptors in the Rat Using [ $^3H$ ]MK912 and Subtype-Selective Drugs. *Brain Res.* **1997**, *770*, 261–266.
- (15) Uhlen, S.; Wikberg, J. E. Delineation of Rat Kidney  $\alpha_{2A}$ - and  $\alpha_{2B}$ -Adrenoceptors with [ $^3H$ ]RX821002 Radioligand Binding: Computer Modelling Reveals that Guanfacine Is an  $\alpha_{2A}$ -Selective Compound. *Eur. J. Pharmacol.* **1991**, *202*, 235–243.
- (16) MacDonald, E.; Kobilka, B. K.; Scheinin, M. Gene Targeting-Homing in on  $\alpha_2$ -Adrenoceptor-Subtype Function. *Trends Pharmacol. Sci.* **1997**, *18*, 211–219.
- (17) Kable, J. W.; Murrin, L. C.; Bylund, D. B. In Vivo Gene Modification Elucidates Subtype-Specific Functions of  $\alpha_2$ -Adrenergic Receptors. *J. Pharmacol. Exp. Ther.* **2000**, *293*, 1–7.
- (18) MacMillan, L. B.; Hein, L.; Smith, M. S.; Piascik, M. T.; Limbird, L. E. Central Hypotensive Effects of the  $\alpha_{2A}$ -Adrenergic Receptor Subtype. *Science* **1996**, *273*, 801–803.
- (19) Lakhani, P. P.; MacMillan, L. B.; Guo, T. Z.; McCool, B. A.; Lovinger, D. M.; Maze, M.; Limbird, L. E. Substitution of a Mutant  $\alpha_{2A}$ -Adrenergic Receptor via “hit and run” Gene Targeting Reveals the Role of This Subtype in Sedative, Analgesic, and Anesthetic-Sparing Responses in vivo. *Proc. Natl. Acad. Sci. U.S.A.* **1997**, *94*, 9950–9955.
- (20) Hunter, J. C.; Fontana, D. J.; Hedley, L. R.; Jasper, J. R.; Lewis, R.; Link, R. E.; Secchi, R.; Sutton, J.; Eglen, R. M. Assessment of the Role of  $\alpha_2$ -Adrenoceptor Subtypes in the Antinociceptive, Sedative and Hypothermic Action of Dexmedetomidine in Transgenic Mice. *Br. J. Pharmacol.* **1997**, *122*, 1339–1344.
- (21) Janumpalli, S.; Butler, L. S.; MacMillan, L. B.; Limbird, L. E.; McNamara, J. O. A Point Mutation (D79N) of the  $\alpha_{2A}$  Adrenergic Receptor Abolishes the Antiepileptogenic Action of Endogenous Norepinephrine. *J. Neurosci.* **1998**, *18*, 2004–2008.
- (22) Stone, L. S.; MacMillan, L. B.; Kitto, K. F.; Limbird, L. E.; Wilcox, G. L. The  $\alpha_{2A}$  Adrenergic Receptor Subtype Mediates Spinal Analgesia Evoked by  $\alpha_2$  Agonists and Is Necessary for Spinal Adrenergic-Opioid Synergy. *J. Neurosci.* **1997**, *17*, 7157–7165.
- (23) (a) Franowicz, J. S.; Arnsten, A. F. The  $\alpha_{2A}$  Noradrenergic Agonist, Guanfacine, Improves Delayed Response Performance in Young Adult Rhesus Monkeys. *Psychopharmacol.* **1998**, *136*, 8–14. (b) Avery, R. A.; Franowicz, J. S.; Studholme, C.; van Dyck, C. H.; Arnsten, A. F. The  $\alpha_{2A}$ -Adrenoceptor Agonist, Guanfacine, Increases Regional Cerebral Blood Flow in Dorsolateral Prefrontal Cortex of Monkeys Performing a Spatial Working Memory Task. *Neuropsychopharmacol.* **2000**, *23*, 240–249.
- (24) Link, R. E.; Desai, K.; Hein, L.; Stevens, M. E.; Chruscinski, A.; Bernstein, D.; Barsh, G. S.; Kobilka, B. K. Cardiovascular Regulation in Mice Lacking  $\alpha_2$ -Adrenergic Receptor Subtypes b and c. *Science* **1996**, *273*, 803–805.
- (25) Makaritsis, K. P.; Handy, D. E.; Johns, C.; Kobilka, B. K.; Gavras, I.; Gavras, H. Role of the  $\alpha_{2B}$ -Adrenergic Receptor in the Development of Salt-Induced Hypertension. *Hypertension* **1999**, *33*, 14–17.
- (26) Rohrer, D. K.; Kobilka, B. K. Insights from in Vivo Modification of Adrenergic Receptor Gene Expression. *Annu. Rev. Pharmacol. Toxicol.* **1998**, *38*, 351–373.
- (27) Chotani, M. A.; Mitra, S.; Su, B. Y.; Flavahan, S.; Eid, A. H.; Clark, K. R.; Montague, C. R.; Paris, H.; Handy, D. E.; Flavahan, N. A. Regulation of  $\alpha_2$ -Adrenoceptors in Human Vascular Smooth Muscle Cells. *Am. J. Physiol. Heart Circ. Physiol.* **2004**, *286*, 59–67.
- (28) Bucheler, M. M.; Hadamek, K.; Hein, L. Two  $\alpha_2$ -Adrenergic Receptor Subtypes,  $\alpha_{2A}$  and  $\alpha_{2C}$ , Inhibit Transmitter Release in the Brain of Gene-Targeted Mice. *Neuroscience* **2002**, *109*, 819–826.
- (29) Bjorklund, M.; Sirvio, J.; Sallinen, J.; Scheinin, M.; Kobilka, B. K.; Riekkinen, P., Jr.  $\alpha_{2C}$ -Adrenoceptor Overexpression Disrupts Execution of Spatial and non-Spatial Search Patterns. *Neuroscience* **1999**, *88*, 1187–1198.
- (30) Tanila, H.; Mustonen, K.; Sallinen, J.; Scheinin, M.; Riekkinen, P. Jr. Role of  $\alpha_{2C}$ -Adrenoceptor Subtype in Spatial Working Memory as Revealed by Mice with Targeted Disruption of the  $\alpha_{2C}$ -Adrenoceptor Gene. *Eur. J. Neurosci.* **1999**, *11*, 599–603.
- (31) Sallinen, J.; Haapalinna, A.; Viitamaa, T.; Kobilka, B. K.; Scheinin, M. Adrenergic  $\alpha_{2C}$ -Receptors Modulate the Acoustic Startle Reflex, Prepulse Inhibition, and Aggression in Mice. *J. Neurosci.* **1998**, *18*, 3035–3042.
- (32) Sallinen, J.; Haapalinna, A.; Viitamaa, T.; Kobilka, B. K.; Scheinin, M. D-Amphetamine and L-5-Hydroxytryptophan-Induced Behaviours in Mice with Genetically-Altered Expression of the  $\alpha_{2C}$ -Adrenergic Receptor Subtype. *Neuroscience* **1998**, *86*, 959–965.
- (33) Fairbanks, C. A.; Stone, L. S.; Kitto, K. F.; Nguyen, H. O.; Posthumus, I. J.; Wilcox, G. L.  $\alpha_{2C}$ -Adrenergic Receptors Mediate Spinal Analgesia and Adrenergic-Opioid Synergy. *J. Pharm. Exp. Ther.* **2002**, *300*, 282–290.

- (34) Pigni, M.; Bousquet, P.; Carotti, A.; Dontenwill, M.; Giannella, M.; Moriconi, R.; Piergentili, A.; Quaglia, W.; Tayebati, S. K.; Brasili, L. Imidazoline Receptors: Qualitative Structure–Activity Relationship and Discovery of Tracizoline and Benzazoline. Two Ligands with High Affinity and Unprecedented Selectivity. *Bioorg. Med. Chem.* **1997**, *5*, 833–841.
- (35) Pigni, M.; Quaglia, W.; Gentili, F.; Marucci, G.; Cantalamessa, F.; Franchini, S.; Sorbi, C.; Brasili, L. Structure–Activity Relationship at  $\alpha$ -Adrenergic Receptors within a Series of Imidazoline Analogues of Cirazoline. *Bioorg. Med. Chem.* **2000**, *8*, 883–888.
- (36) Gentili, F.; Bousquet, P.; Brasili, L.; Caretto, M.; Carrieri, A.; Dontenwill, M.; Giannella, M.; Marucci, G.; Perfumi, M.; Piergentili, A.; Quaglia, W.; Rascente, C.; Pigni, M.  $\alpha_2$ -Adrenoreceptors Profile Modulation and High Antinociceptive Activity of (S)-(-)-2-[1-(Biphenyl-2-yloxy)ethyl]4,5-dihydro-1H-imidazole. *J. Med. Chem.* **2002**, *45*, 32–40.
- (37) Gentili, F.; Bousquet, P.; Brasili, L.; Dontenwill, M.; Feldman, J.; Ghelfi, F.; Giannella, M.; Piergentili, A.; Quaglia, W.; Pigni, M. Imidazoline Binding Sites (IBS) Profile Modulation: Key Role of the Bridge in Determining I<sub>1</sub>-IBS or I<sub>2</sub>-IBS Selectivity within a Series of 2-Phenoxymethylimidazoline Analogues. *J. Med. Chem.* **2003**, *46*, 2169–2176.
- (38) Lalchandani, S. G.; Zhang, X.; Hong, S. S.; Liggett, S. B.; Li, W.; Moore II, B. M.; Miller, D. D.; Feller, D. R. Medetomidine Analogs as Selective Agonists for the Human  $\alpha_2$ -Adrenoreceptors. *Science* **2004**, *67*, 87–96.
- (39) Moldereings, G. J. Imidazoline Receptors: Basic Knowledge, Recent Advances and Future Prospects for Therapy and Diagnosis. *Drugs Future* **1997**, *22*, 757–772.
- (40) Eglén, R. M.; Hudson, A. L.; Kendall, D. A.; Nutt, D. J.; Morgan, N. G.; Wilson, V. G.; Dillon, M. P. “Seeing through a Glass Darkly”: Casting Light on Imidazoline “T” Sites. *Trends Pharmacol. Sci.* **1998**, *19*, 381–390.
- (41) Magnien, E.; Testa, F.; Shapiro, S. L. Substituted 2-Phenoxypionic and -butyric Acids and Derivatives. *J. Med. Chem.* **1966**, *9*, 449–450.
- (42) Miyaura, N.; Yanagi, T.; Suzuki, A. The Palladium-Catalyzed Cross-Coupling Reaction of Phenylboronic Acid with Haloarenes in the Presence of Bases. *Synth. Commun.* **1981**, *11*, 513–519.
- (43) (a) Colbert, J. C.; Lacy, R. M. The Effect of Substituent Groups upon the Course of the Condensation Reaction between Benzenediazonium Salts and Phenols. *J. Am. Chem. Soc.* **1946**, *68*, 270–271. (b) Downie, I. M.; Heaney, H.; Kemp, G.; King, D.; Wosley, M. Cyclisation Reactions of 2-Substituted Biphenyl-2'-yldiazonium Salts Leading to O-Alkyldibenzofuranium and S-Alkyldibenzothiophenium Salts: Modified Meerwein Reagents. *Tetrahedron* **1992**, *48*, 4005–4016.
- (44) Deschamps, B.; Seyden-Penne, J. Effet de Solvant sur la Stéréochimie de la Réaction de Darzens. III. Etude de la Condensation du Chloracetonitrile et des Aldehydes Aromatiques en Milieu Basique. *Tetrahedron* **1971**, *27*, 3959–3964.
- (45) Cullen, B. R. Use of Eukaryotic Expression Technology in the Functional Analysis of Cloned Genes. *Methods Enzymol.* **1987**, *152*, 684–704.
- (46) Devedjian, J.-C.; Esclapez, F.; Denis-Pouxviel, C.; Paris, H. Further Characterization of Human  $\alpha_2$ -Adrenoreceptor Subtypes: [<sup>3</sup>H]-RX 821002 Binding and Definition of Additional Selective Drugs. *Eur. J. Pharmacol.* **1994**, *252*, 43–49 and references therein.
- (47) Cheng, Y. C.; Prusoff, W. H. Relationship Between the Inhibition Constant (K<sub>i</sub>) and the Concentration of Inhibitor which Causes 50% Inhibition (I<sub>50</sub>) of an Enzymatic Reaction. *Biochem. Pharmacol.* **1973**, *22*, 3099–3108.
- (48) Pihlavisto, M.; Scheinin, M. Functional Assessment of Recombinant Human  $\alpha_2$ -Adrenoreceptor Subtypes with Cytosensor Microphysiometry. *Eur. J. Pharmacol.* **1999**, *385*, 247–253.
- (49) Bairoch, A.; Apweiler, R. The SWISS-PROT Protein Sequence Data Bank and Its Supplement TrEMBL in 1998. *Nucleic Acids Res.* **1998**, *26*, 38–42.
- (50) Ballesteros, J. A.; Weinstein, H. Integrated Methods for the Construction of Three-Dimensional Models and Computational Probing of Structure–Function Relations in G Protein-Coupled Receptors. *Methods Neurosci.* **1995**, *25*, 366–428.
- (51) Li, J.; Edwards, P.; Burghammer, M.; Villa, C.; Schertler, G. F. X. Structure of Rhodopsin in a Trigonal Crystal Form, to be published. The rhodopsin structure (PDB code 1GZM) is available at the following URL <http://www.rcsb.org>.
- (52) Sali, A.; Blundell, T. L. Comparative Protein Modelling by Satisfaction of Spatial Restraints. *J. Mol. Biol.* **1993**, *234*, 779–815.
- (53) Kelley, L.; Gardner, S. P.; Sutcliffe, M. J. An Automated Approach for Clustering an Ensemble of NMR-Derived Protein Structures into Conformationally Related Subfamilies. *Protein Eng.* **1996**, *9*, 1063–1065.
- (54) Laskowski, R. A.; MacArthur, M. W.; Moss, D. S.; Thornton, J. M. PROCHECK: A Program to Check the Stereochemical Quality of Protein Structures. *J. Appl. Crystallogr.* **1993**, *26*, 283–291.
- (55) McMartin, C.; Bohacek, R. S. QXP: Powerful, Rapid Computer Algorithms for Structure-Based Drug Design. *J. Comput. Aided Mol. Des.* **1997**, *11*, 333–344.
- (56) Wang, C. D.; Buck, M. A.; Fraser, C. M. Site-Directed Mutagenesis of  $\alpha_{2A}$ -Adrenergic Receptors: Identification of Amino Acids Involved in Ligand Binding and Receptor Activation by Agonists. *Mol. Pharmacol.* **1991**, *40*, 168–179.
- (57) Hansch, C.; Leo, A.; Unger, S. H.; Kim, K. H.; Nikaitani, D.; Lien, E. J. “Aromatic” Substituent Constants for Structure–Activity Correlations. *J. Med. Chem.* **1973**, *16*, 1207–1216.
- (58) Schaak, S.; Cayla, C.; Lymperopoulos, A.; Flordellis, C.; Cussac, D.; Denis, C.; Paris, H. Transcriptional Down-Regulation of the Human  $\alpha_{2C}$ -Adrenergic Receptor by cAMP. *Mol. Pharmacol.* **2000**, *58*, 821–827.
- (59) Ballesteros, J. A.; Jensen, A. D.; Liapakis, G.; Rasmussen, S. G.; Shi, L.; Gether, U.; Javitch, J. A. Activation of the  $\beta_2$ -Adrenergic Receptor Involves Disruption of an Ionic Lock between the Cytoplasmic Ends of Transmembrane Segments 3 and 6. *J. Biol. Chem.* **2001**, *276*, 29171–29177.
- (60) Porter, J. E.; Hwa, J.; Perez, D. M. Activation of the  $\alpha_{1B}$ -Adrenergic Receptor is Initiated by Disruption of an Interhelical Salt Bridge Constraint. *J. Biol. Chem.* **1996**, *271*, 28318–28323.
- (61) Strader, C. D.; Candelore, M. R.; Hill, W. S.; Sigal, I. S.; Dixon, R. A. Identification of Two Serine Residues Involved in Agonist Activation of the  $\beta$ -Adrenergic Receptor. *J. Biol. Chem.* **1989**, *264*, 13572–13578.
- (62) Hwa, J.; Perez, D. M. The Unique Nature of the Serine Interactions for  $\alpha_1$ -Adrenergic Receptor Agonist Binding and Activation. *J. Biol. Chem.* **1996**, *271*, 6322–6327.
- (63) Carrieri, A.; Centeno, N. B.; Rodrigo, J.; Sanz, F.; Carotti, A. Theoretical Evidence of a Salt Bridge Disruption as the Initiating Process for the  $\alpha_{1D}$ -Adrenergic Receptor Activation: A Molecular Dynamics and Docking Study. *Proteins* **2001**, *43*, 382–394.
- (64) Shi, L.; Liapakis, G.; Xu, R.; Guarnieri, F.; Ballesteros, J. A.; Javitch, J. A.  $\beta_2$ -Adrenergic Receptor Activation. Modulation of the Proline Kink in Transmembrane 6 by a Rotamer Toggle Switch. *J. Biol. Chem.* **2002**, *277*, 40989–40996.
- (65) Schaak, S.; Devedjian, J. C.; Paris, H. Use of Eukaryotic Vectors for the Expression of Adrenergic Receptors. *Methods Mol. Biol.* **2000**, *126*, 189–206.
- (66) Bradford, M. M. A Rapid and Sensitive Method for the Quantitation of Microgram Quantities of Protein Utilizing the Principle of Protein–Dye Binding. *Anal. Biochem.* **1976**, *72*, 248–254.

JM0408215